*Journal of Zhejiang University-SCIENCE A 2025 26(9):832-852*
www.jzus.zju.edu.cn; www.springer.com/journal/11582
E-mail: jzus_a@zju.edu.cn

**Review**

https://doi.org/10.1631/jzus.A2500056



# Efficient and stable perovskite light-emitting diodes

Zhuoyue GU[1,2*], Suhui ZHANG[1,2*], Wentao XIONG[1,2✉], Baodan ZHAO[1,2✉], Dawei DI[1,2,3✉]

[1]*State Key Laboratory of Extreme Photonics and Instrumentation, College of Optical Science and Engineering, Zhejiang University, Hangzhou 310027, China*
[2]*International Research Center for Advanced Photonics, Zhejiang University, Hangzhou 310027, China*
[3]*Zhejiang University-University of Illinois Urbana-Champaign Institute, Zhejiang University, Jiaxing 314400, China*

**Abstract:** Perovskite light-emitting diodes (PeLEDs) have shown outstanding potential in next-generation lighting and display owing to the advantages of broad spectral tunability, excellent color purity, high photoluminescence quantum yields (PLQYs), and low processing cost. Device efficiency and stability are crucial indicators to evaluate whether a PeLED can meet commercial application requirements. In this review, we first discuss strategies for achieving high external quantum efficiencies (EQEs), including controlling charge injection and balance, enhancing radiative recombination, and improving light outcoupling efficiency. Next, we review recent advances in operational stability of PeLEDs and emphasize the mechanisms of degradation in PeLEDs, including ion migration, structural transformations, chemical interactions, and thermal degradation. Through detailed analysis and discussion, this review aims to facilitate progress and innovation in highly efficient and stable PeLEDs, which have significant promise for display and solid-state lighting technologies, as well as other emerging applications.

**Key words:** Perovskite; Light-emitting diodes; External quantum efficiency (EQE); Stability

## 1 Introduction

In the pursuit of innovative light sources to revolutionize display and lighting technologies, perovskite light-emitting diodes (PeLEDs) have emerged as a promising candidate (Tan et al., 2014; Cho et al., 2015). They possess advantages of broad spectral tunability, excellent color purity, high photoluminescence quantum yields (PLQYs), and low processing cost. Since the first report of room-temperature electroluminescence (EL) in halide perovskite (Tan et al., 2014), the field has witnessed a remarkable growth.

Through improvements in emissive perovskites and device structures, the external quantum efficiencies (EQEs) of PeLEDs with emission wavelengths varying from green to near-infrared (NIR) have exceeded 30% (Feng et al., 2024; Li MM et al., 2024; Sun et al., 2024). And the EQEs of blue PeLEDs have surpassed 20% (Gao et al., 2024). Despite these encouraging improvements in efficiency for PeLEDs, operational stability remains a significant challenge. A recent breakthrough showcased efficient NIR PeLEDs with a remarkable operational lifetime of 32675 h at a current density of 3.2 mA/cm$^2$ (Guo et al., 2022). However, visible PeLEDs still suffer from poor stability, which restricts their application in commercial display technologies.

In this review, we consider paths for further development in efficiency and stability for PeLEDs. First, we focus on strategies to create highly efficient PeLEDs, including controlling charge injection and balance, enhancing radiative recombination, and improving light outcoupling. Subsequently, we conclude the best-performing devices in terms of stability, and discuss degradation mechanisms in PeLEDs (Fig. 1). By analyzing the efficiency and stability challenges faced by PeLEDs, we expect that further insights could be gained for improved device fabrication, facilitating commercial applications.

✉ Dawei DI, daweidi@zju.edu.cn
Baodan ZHAO, baodanzhao@zju.edu.cn
Wentao XIONG, wtxiong@zju.edu.cn
* The two authors contributed equally to this work
Dawei DI, https://orcid.org/0000-0003-0703-2809

Received Feb. 25, 2025; Revision accepted May 22, 2025; Crosschecked July 31, 2025

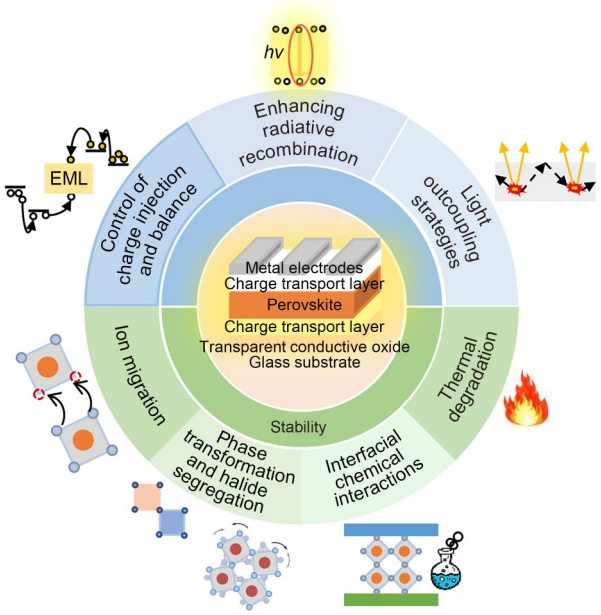


**Fig. 1 Strategies for high efficiency and factors of instability in PeLEDs. *h* is the Planck constant; *v* is the frequency of light. References to color refer to the online version of this figure**

## 2 Creating highly efficient PeLEDs

Typically, PeLED devices feature a sandwich-like structure, where the central perovskite emissive layer (EML) is flanked by the electron-transport layer (ETL) and the hole-transport layer (HTL). Similar to the device architectures of organic light emitting diodes (OLEDs), the structures of PeLEDs can be classified into regular (p-i-n) or inverted (n-i-p) types (Zhao BD et al., 2020; Guo et al., 2022). The most important metric for the efficiency of PeLEDs is the external quantum efficiency ($E_e$), which is the ratio between the number of emitted photons and the injected carriers per unit time (Cao et al., 2018; Xu et al., 2019).

The $E_e$ of PeLEDs can be determined by:

$$E_e = E_i \times f_{outcoupling} = f_{balance} \times f_{e\text{–}h} \times \eta_{rad} \times f_{outcoupling}, \quad (1)$$

where $E_i$ is the internal quantum efficiency (IQE); $f_{balance}$ is the factor of charge injection balance; $f_{e\text{–}h}$ is the probability of producing a correlated electron–hole (e–h) pair generated from each pair of injected carriers; $\eta_{rad}$ is the radiative recombination efficiency of each electron–hole pair; $f_{outcoupling}$ is the optical outcoupling efficiency (Stranks et al., 2019; Zhao et al., 2023).

According to this formula, building PeLEDs with higher EQE requires enhancing both IQE and $f_{outcoupling}$. IQE is determined by $f_{balance}$, $f_{e\text{–}h}$, and $\eta_{rad}$. The $f_{balance}$ can be improved by optimizing energy level alignment (Zhao and Tan, 2020; Zhao BD et al., 2020) and charge transport properties (Zhao et al., 2018). Main strategies for improving $f_{e\text{–}h}$ include forming charge-confinement structures (Wang et al., 2016; Yuan et al., 2016), and reducing the dielectric constants to enhance Coulomb interactions (Stranks et al., 2019; Jiang et al., 2021). For perovskite emitters, $\eta_{rad}$ is determined by $\eta_{rad} = k_2N^2/(k_1N + k_2N^2 + k_3N^3)$, where $k_1$ is the trap-assisted recombination rate, $k_2$ is the rate of band-to-band radiative recombination, $k_3$ is the Auger recombination constant, and $N$ is the carrier density (Stranks et al., 2019; Zhao et al., 2023). Enhancing $f_{outcoupling}$ requires suppressing the light losses from the substrate and waveguide modes, so the light management strategies are essential for maximizing photon extraction (Cho et al., 2020; Zhao et al., 2023).

### 2.1 Control of charge injection and balance

When applying a forward bias between the electrodes of PeLEDs, the electrons and holes migrate through the charge-transport layer (CTL) to the EML, where they recombine to emit light (Tan et al., 2014). Energy level barrier and interface mismatches between electrodes and EMLs can hamper charge injection. Therefore, to achieve efficient charge injection, it is crucial to ensure proper energy level alignment so as to minimize the injection barrier. Also, ETL with deep highest occupied molecular orbitals (HOMO) and HTL with shallow lowest unoccupied molecular orbitals (LUMO) can block electrons and holes, respectively, confining recombination to the perovskite layer (Fig. 2a) (Tan et al., 2014; Li et al., 2025).

To function efficiently, PeLEDs require not only effective charge carrier injection but also a balanced distribution of electrons and holes. It is essential to minimize charge imbalance losses, which can occur if one carrier type is in excess (Fig. 2b) (Zou et al., 2019; Chen ZM et al., 2021).

#### 2.1.1 Optimizing energy level alignment

Due to the significant energy level barrier between the electrode and the perovskite layer, selecting appropriate CTLs to optimize energy level alignment is essential for efficient charge carrier injection. The commonly

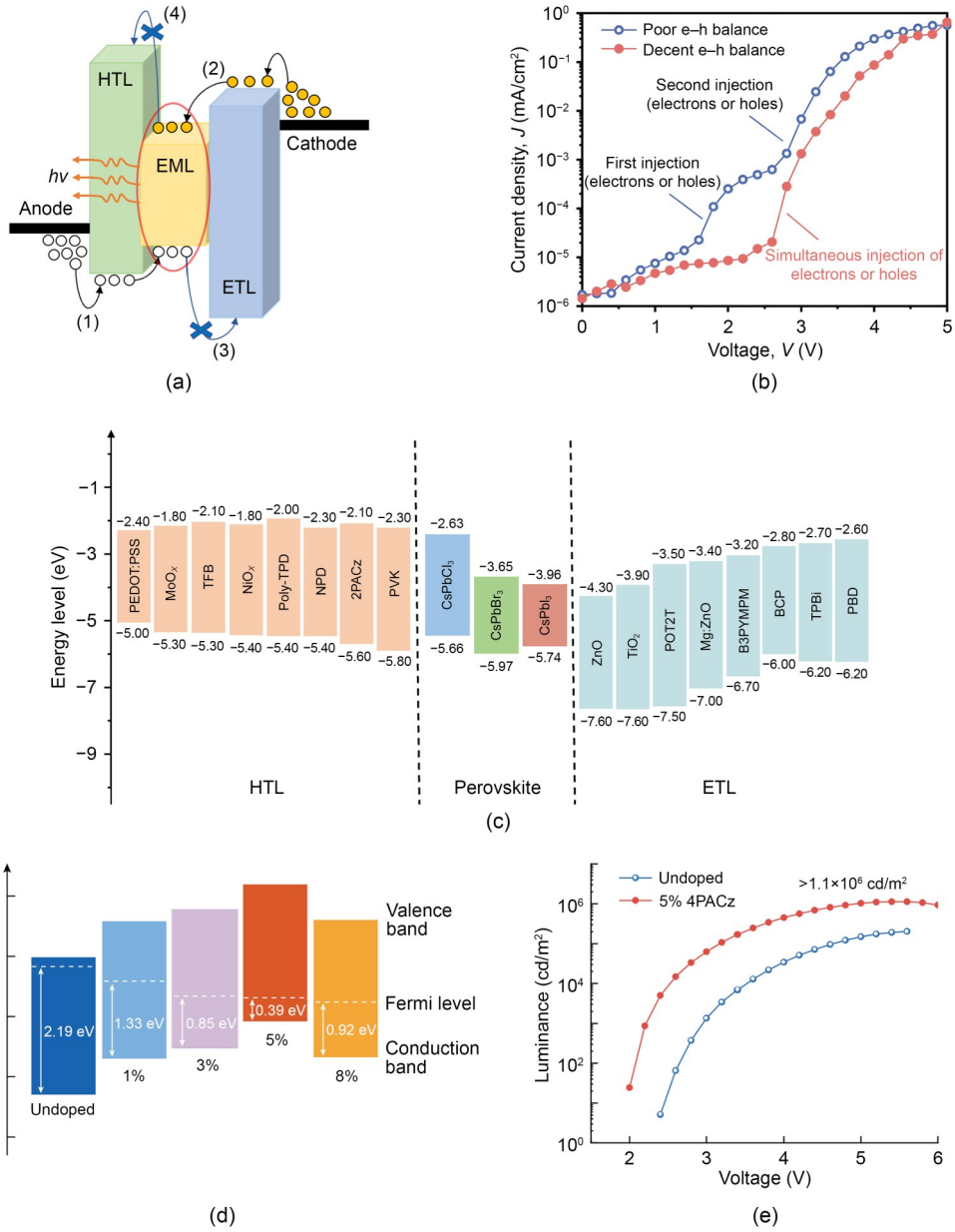


**Fig. 2 (a) Diagram of a PeLED with a "regular" structure: (1) hole injection; (2) electron injection; (3) hole blocking; (4) electron blocking (reprinted from (Li et al., 2025), Copyright 2025, with permission from Springer Nature); (b) *J*–*V* curves for poor and decent electron-hole balances in PeLEDs (reprinted from (Chen ZM et al., 2021), Copyright 2021, with permission from Institute of Physics Publishing); (c) energy levels of commonly used ETLs and HTLs for $CsPbCl_3$, $CsPbBr_3$, and $CsPbI_3$ perovskite layers (reprinted from (Li et al., 2025), Copyright 2025, with permission from Springer Nature); (d) energy levels of the perovskite samples with different doping concentrations (reprinted from (Xiong et al., 2024), Copyright 2024, with permission from Springer Nature); (e) luminance–voltage curves of the perovskite samples (reprinted from (Xiong et al., 2024), Copyright 2024, with permission from Springer Nature). TFB: poly(9,9-dioctylfluorene-co-N-(4-(3methylpropyl))diphenylamine; NPD: N,N′-bis-(1-naphthalenyl)-N,N′-bis-phenyl-(1,1′-biphenyl)-4,4′-diamine; 2PACz: (2-(9H-carbazol-9-yl)ethyl)phosphonic acid; POT2T: 2,4,6-tris[3-(diphenylphosphinyl)phenyl]-1,3,5-triazine; B3PYMPM: 4,6-bis(3,5-di-3-pyridylphenyl)-2-methylpyrimidine; BCP: 2,9-dimethyl-4,7-diphenyl-1,10-phenanthrolin; TPBi: 1,3,5-tris(1-phenyl-1H-benzimidazol-2-yl) benzene; PBD: 2-(4-Biphenylyl)-5-phenyloxadiazole. References to color refer to the online version of this figure**

used CTLs in PeLEDs are summarized in Fig. 2c. To enhance charge injection efficiency, designing a well-constructed energy level cascade is an effective strategy (Zou et al., 2020; Yu et al., 2022). By successively depositing multiple layers of HTLs—poly(3,4-ethylenedioxythiophene)-poly(styrenesulfonate) (PEDOT:PSS),

poly(N,N′-bis-4-butylphenyl-N,N′-bisphenyl (poly-TPD), and poly(N-vinylcarbazole) (PVK)—on the indium tin oxide (ITO) substrate, an energy cascade can be created to optimize hole injection. The HOMO levels progressively deepened from −5.00 eV (PEDOT:PSS) to −5.80 eV (PVK), aligning closely with the valance band maximum (VBM) of $CsPbBr_3$ (−5.97 eV), and thus reducing the hole injection barrier. This alignment led to improved device efficiency and reduced EQE roll-off (Zou et al., 2020).

Introducing mixed organic CTLs is also an effective approach to adjust energy band structures. By incorporating the electron-accepting molecule 1,3,5-tris(bromomethyl) benzene (TBB) into HTL (poly-TPD), energy level alignment can be improved. Adjusting the concentration of TBB deepens the LUMO level of the mixed HTL from −5.10 eV to −5.42 eV, better aligning it with the VBM of the green EML (Wang HR et al., 2020).

#### 2.1.2 Balancing the charge transport

When excess electron (or hole) injection occurs, this imbalance can be corrected by either impeding the electron (or hole) transport, or accelerating the transport of holes (or electrons) (Fakharuddin et al., 2019). For example, more electrons can be injected from the ETL than holes from the HTL, leading to an uneven spatiotemporal distribution of holes and electrons across the device structure (Wang et al., 2019). Balancing the charge transport is important for maintaining charge injection balance.

Introducing an insulation layer on one side of PeLEDs is a typical strategy for balancing charge transport, which improves the carrier utilization and leads to efficiency improvement. It was reported that insulating polymethyl methacrylate (PMMA) can be introduced to separate the ETL and the cathode. The insulating PMMA effectively impeded the excess electron flow, balancing the electron and hole injection, and moving the carrier recombination region towards the central region of the EML (Lin et al., 2018).

While the introduction of an insulating layer can reduce excessive electron injection, it may also result in electron accumulation and increased Joule heating. Regulating the carrier polarity and concentration within the perovskite layer is also an effective way to optimize the device structure, ensuring efficient carrier injection and balance. By introducing a phosphonic acid molecular dopant with strong electron-withdrawing properties, (4-(9H-carbazol-9-yl)butyl)phosphonic acid (4PACz), a transition from n-type to p-type conductivity in the perovskite semiconductor can be achieved (Fig. 2d), significantly enhancing hole transport and shifting the carrier recombination region. PeLEDs based on the p-type perovskite achieved ultra-high luminance (>$1.1\times10^6$ cd/m$^2$) (Fig. 2e), EQE (28.4%), and a record-high energy conversion efficiency for visible PeLEDs (23.1%) (Xiong et al., 2024), demonstrating the importance of electrical doping in perovskites for improving charge transport in PeLEDs.

### 2.2 Enhancing radiative recombination

The charge carrier recombination kinetics dependency on carrier density can be described by:

$$-\frac{\mathrm{d}N(t)}{t}=k_1N+k_2N^2+k_3N^3. \tag{2}$$

The definitions of $k_1$, $k_2$, $k_3$ and $N$ are the same as those mentioned earlier, and $t$ is the time (Fig. 3a) (Quan et al., 2017; Luo et al., 2019; Stranks et al., 2019). Due to the relatively small exciton binding energy (about 10 meV), excitons in three-dimensional (3D) perovskites can easily dissociate into free carriers, which can be captured by defect centers at low carrier densities; this leads to enhanced trap-assisted recombination (Stranks et al., 2019). Simulation results show that low $k_2$ is a significant factor limiting the carrier recombination of 3D perovskites (Fig. 3b) (Cao et al., 2018). A recent study demonstrated that incorporating dual additives into $FAPbI_3$ ($CH(NH_2)_2PbI_3$, and $FA^+$ corresponds to $CH(NH_2)_2^+$) perovskite leads to higher exciton binding energy, which effectively accelerates radiative recombination and thus achieves a remarkable peak EQE of 32% in NIR PeLEDs (Fig. 3c) (Li MM et al., 2024).

Trap-assisted recombination and Auger recombination are also significant factors limiting efficiency improvement in PeLEDs. At moderate to low carrier densities, trap-assisted recombination is the main cause of non-radiative losses. It dominates at carrier density $N<5\times10^{16}$ cm$^{-3}$, making trap passivation crucial for improving PeLED performance (Fig. 3d) (Richter et al., 2016; Fakharuddin et al., 2022). At higher carrier densities ($N>10^{18}$ cm$^{-3}$), enhancing the Auger recombination causes efficiency losses (Richter et al., 2016; Xing et al., 2017).

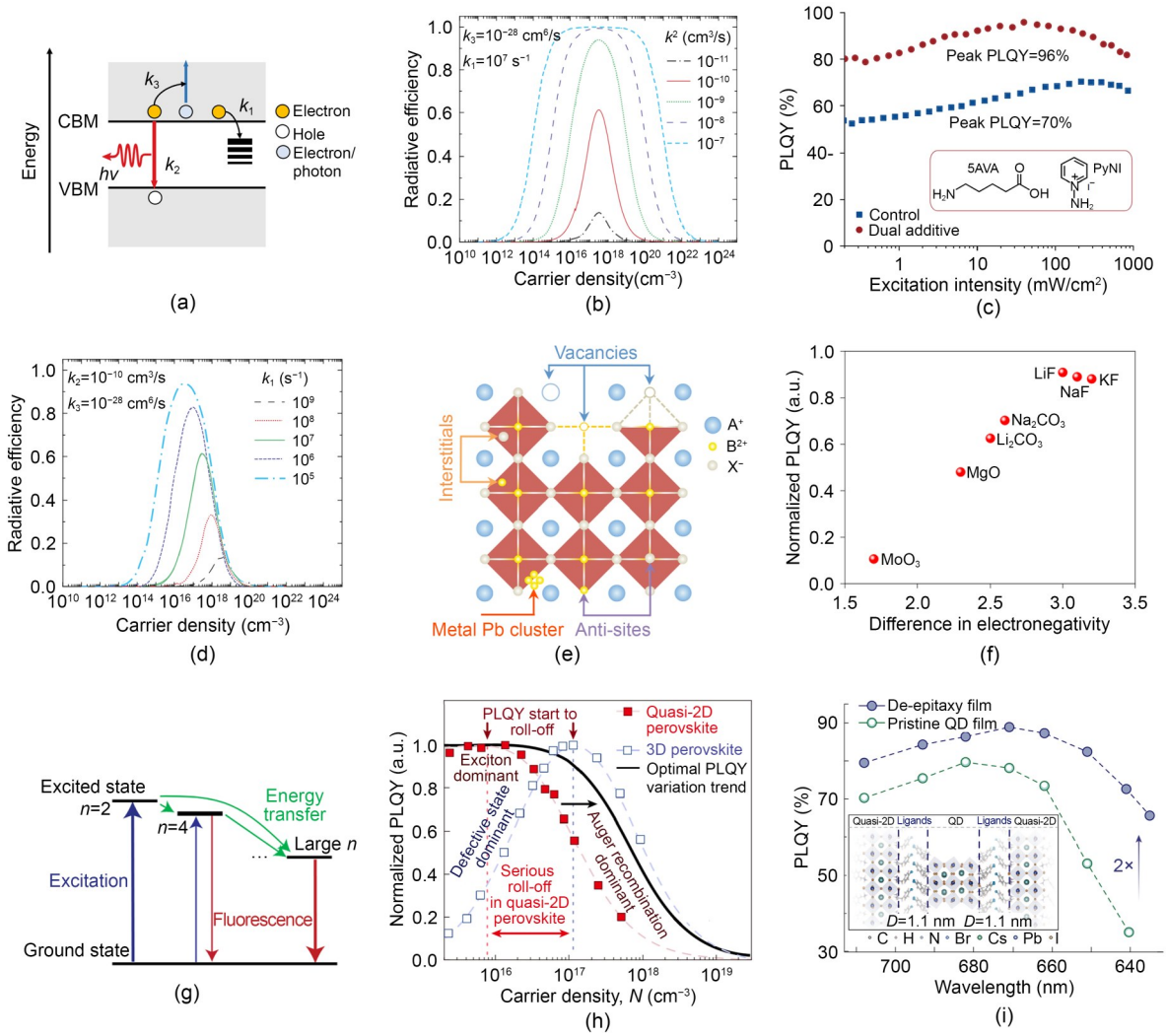


**Fig. 3 (a) Recombination pathways in 3D perovskite (reprinted from (Quan et al., 2017), Copyright 2017, with permission from American Chemical Society); (b) relationship between radiative efficiency and carrier density under different band-to-band radiative recombination coefficients $k_2$ (reprinted from (Xing et al., 2017), Copyright 2017, with permission from Springer Nature); (c) excitation-intensity-dependent PLQYs of control and dual-additive perovskites (reprinted from (Li MM et al., 2024), Copyright 2024, with permission from Springer Nature); (d) relationship between radiative efficiency and carrier density under different trap-assisted recombination coefficients $k_1$ (reprinted from (Xing et al., 2017), Copyright 2017, with permission from Springer Nature); (e) point defects of perovskites including interstitial defects, vacancy defects, anti-site substitution defects, and metal Pb clusters (reprinted from (Liu XK et al., 2021), Copyright 2021, with permission from Springer Nature); (f) normalized PLQYs of perovskite layers deposited on a range of interfacial materials with differences in electronegativity of the chemical bonds (reprinted from (Zhao BD et al., 2020), Copyright 2020, with permission from Springer Nature); (g) schematic of cascade energy transfer in MQWs (reprinted from (Wang et al., 2016), Copyright 2016, with permission from Springer Nature); (h) normalized PLQYs of quasi-2D perovskite and 3D perovskite films as a function of carrier density (reprinted from (Jiang et al., 2021), Copyright 2021, with permission from Springer Nature); (i) PLQYs of different-sized pristine quantum dot (QD) films and $CsPbI_3$ QD de-epitaxy films (reprinted from (Wei et al., 2025), Copyright 2025, with permission from Springer Nature). CBM is the conduction band minimum; PyNI is the 1-aminopyridinium iodide; 5AVA is the 5-aminovaleric acid; $n$ is the number of semiconducting monolayer sheets within the two organic insulating layers; $D$ is the gap distance between QD and quasi-2D components. References to color refer to the online version of this figure**

### 2.2.1 Defect passivation

To limit trap-assist recombination, it is critical to inhibit the formation of defects in perovskite crystal, including interstitial defects, vacancy defects, and anti-site substitution defects (Fig. 3e) (Ball and Petrozza, 2016; Liu XK et al., 2021). This is often achieved by the incorporation of small-molecule (Ban et al., 2018)

and polymeric (Zhao et al., 2018) passivators through direct addition to perovskite precursors, or post treatments on crystallized perovskites (Nenon et al., 2018; Xu et al., 2019). Numerous agents or ligands have proven effective at decreasing the defect density of perovskites, such as Lewis acid/base moieties, organic components with positive or negative charges, and alkali metal ions (Lee et al., 2019; Liu XK et al., 2021; Shen et al., 2023).

The deep-lying traps leading to efficiency loss are thought to mainly stem from undercoordinated lead, including $Pb^{2+}$ and $Pb^{0}$ (Chen et al., 2019). Lewis bases functional groups, including phosphine oxide (P=O), carboxyl (–COOH) and carbonyl (C=O), are widely used to passivate $Pb^{2+}$ by donating lone electron pairs (Lee et al., 2018; Quan et al., 2020; Ren et al., 2021; Shen et al., 2023). Meanwhile, certain polymers and small molecules with functional groups capable of furnishing lone electron pairs have been used to passivate defects in perovskites, in order to enhance the efficiency and operational stability of PeLEDs. Moreover, alkali metal ions ($Li^{+}$, $K^{+}$, and $Rb^{+}$) can be utilized to passivate defects, thereby optimizing device performance (Li et al., 2020; Guo ZY et al., 2021). A notable example involves the treatment of mixed halide perovskite nanocrystals with the ligands ethylenediaminetetraacetic acid (EDTA) and reduced L-glutathione, which bind strongly to lead atoms on the crystal surface to suppress halide segregation. This approach has yielded highly efficient and color-stable red PeLEDs, which achieved an EQE of 20.3% (Hassan et al., 2021).

Additionally, the effectiveness of multiple-passivator strategies has been reported. For example, the ionic liquid [BMIm]OTf ($C_8H_{15}N_2CF_3SO_3$; $[BMIm]^{+}$ and $OTf^{-}$ correspond to $C_8H_{15}N_2^{+}$ and $CF_3SO_3^{-}$, respectively) was found to act as a crystallization modulator via heterogeneous nucleation, and a multi-site passivator—$[BMIm]^{+}$—binds to uncoordinated $Br^{-}$ while $OTf^{-}$ coordinates with $Pb^{2+}$ defects (Luo et al., 2022). This dual passivation suppresses nonradiative recombination while optimizing the morphology of the perovskite. Furthermore, the role of alkali metal ions was shown to extend beyond simple defect passivation. In quasi-2D perovskites, the relatively large radius of $K^{+}$ was reported to result in weaker Coulomb interactions with the $[PbBr_6]^{4-}$ frames, restricting the formation of high-n phases and promoting the homogeneous distribution of low-n phases, achieving a peak EQE of about 18.2% (Guo ZY et al., 2021).

### 2.2.2 Interfacial modification

Interfacial non-radiative recombination loss plays an equally important (if not more important) role compared to bulk regions in terms of performance improvement of PeLEDs. The perovskite layer is typically deposited on CTL by spin-coating, and differences in the interfacial properties between the two layers can affect the crystallization and morphology of the perovskite layer, thereby leading to current leakage and non-radiative recombination losses.

These shortcomings can be improved through various interface modification methods, including introducing perovskite epitaxial growth templates (Zhang et al., 2022), modifying hydrophobic surfaces (Si et al., 2017; Xiao et al., 2017; Zhao BD et al., 2020), and employing self-assembled monolayers (SAMs) (Xiong et al., 2023; Zhou et al., 2023). As reported, ultrathin polar interfaces like lithium fluoride (LiF) can facilitate the formation of high-quality perovskite films on hydrophobic polymeric CTL (Fig. 3f), which acts as an effective template to form perovskite grains with fewer voids; this can remarkably improve the quality of the perovskite layers (Zhao BD et al., 2020).

### 2.2.3 Dimensionality regulation

In conventional 3D PeLEDs, due to the relatively low exciton binding energy, excitons are prone to being captured by defects, which leads to non-radiative recombination. In contrast, perovskites with low-dimensional and nanocrystalline structures exhibit the quantum confinement effect, which increases the exciton binding energy (Quan et al., 2017; Liu XK et al., 2021). To this end, research into mixed-dimensional perovskite systems featuring multiple quantum well (MQW) structures has been initiated. Through the energy funneling mechanism, carriers are confined within the lower-bandgap perovskite regions, thus improving the local carrier density and enhancing radiative recombination (Fig. 3g) (Wang et al., 2016; Yuan et al., 2016; Cheng et al., 2020).

However, in low-dimensional perovskite systems, the carrier density at the recombination center is significantly higher than in 3D perovskites, leading to more severe Auger recombination and causing PLQY to decline rapidly at a relatively low carrier density threshold. This causes the EQE roll-off to be more pronounced (Fig. 3h) (Jiang et al., 2021). A recent study employed a double-edge contacted epitaxy (de-epitaxy)

heterostructure combining quantum dots (QDs) and quasi-2D $CsPbI_3$ films, which preserves the excellent charge transport properties of the quasi-2D perovskite while enhancing the PLQY of the QDs (Fig. 3i). This approach also improved the stability of the perovskite crystal phase, achieving a peak EQE of 24.6% and high stability in red PeLEDs (Wei et al., 2025).

### 2.3 Light outcoupling strategies

The IQEs of top-performing PeLEDs are currently nearing unity, while approximately 80% of generated photons remain confined within the device due to limited light outcoupling yields (Wang et al., 2016; Lin et al., 2018; Zhao et al., 2018). This limited outcoupling efficiency results from two primary factors: (1) waveguide modes induced by the higher refractive indices of perovskites (about 2.5) compared with commonly used charge transport materials and transparent electrodes (about 1.7–1.8) (Zhao et al., 2018); (2) total light internal reflection across a wide range of angles due to the refractive index mismatch between the device substrate and air (Cho et al., 2020; Zhao et al., 2023).

To improve EQEs of PeLEDs, extracting trapped photons from the device is essential. Strategies to enhance light outcoupling in PeLEDs can be broadly categorized into two approaches: modulation of intrinsic optical properties and optimization of external optical structures (Zhao et al., 2023).

#### 2.3.1 Modulation of intrinsic optical properties

Techniques for modulation of intrinsic optical properties include the reduction of refractive index $n_0$ (Zhao et al., 2018), orientation of transition dipole moments (TDMs) (Fieramosca et al., 2018; Shen et al., 2019; Proppe et al., 2020; Zou and Lin, 2020; Cho and Greenham, 2021; Cui et al., 2021), and photon recycling (Cho et al., 2020).

According to the ray optics limit of $(1/2)n_0^2$, the reduction of $n_0$ can increase $f_{\text{outcoupling}}$ for planar devices (Richter et al., 2016). For typical 3D perovskites ($n_0\approx$ 2.5), the outcoupling efficiency is around 10%. To reduce $n_0$, creating perovskite-polymer bulk heterostructures (PPBH) by introducing polymers into the perovskite emissive layers is effective. This approach results in $n\approx1.9$ and improves the $f_{\text{outcoupling}}$ to about 21% (Fig. 4a) in NIR PeLEDs (Zhao et al., 2018).

The orientation of TDMs significantly influences photon extraction processes, with horizontally oriented TDMs enhancing the light extraction. The ratio of horizontal TDMs can be adjusted by engineering the perovskite nanostructures (Fieramosca et al., 2018; Shen et al., 2019; Proppe et al., 2020; Cui et al., 2021). For PeLEDs based on nanoplatelets, the ratio of horizontal TDMs was reported as about 84%, and the $f_{\text{outcoupling}}$ was 31% (Cui et al., 2021). The orientations of TDMs can also be tuned by solution-processed polycrystalline perovskite films (Fig. 4b) (Cui et al., 2021; Zhao et al., 2023). Meanwhile, a slightly preferred orientation (horizontal dipole ratio of 0.41) can lead to a $f_{\text{outcoupling}}$ value of over 20%, and a maximum EQE of 36% (Zou and Lin, 2020).

Photon recycling enhances the light outcoupling by randomizing the directions of trapped photons through the reabsorption of photons and re-emitting processes (Richter et al., 2016; Stranks et al., 2019; Bowman et al., 2020; Cho et al., 2020; Zhao et al., 2023). A typical approach for improving the photon recycling contribution is increasing the thickness of perovskite film (Fig. 4c) (Cho et al., 2020). Notably, using a relatively thick (about 2.2 μm) emissive layer led to a high EQE exceeding 15%, while the calculated $f_{\text{outcoupling}}$ value based on the conventional model was only around 4.3% (Chen J et al., 2021).

The theoretical EQE $E_{\text{PR}}$ of a PeLED with photon recycling (PR) is given by:

$$E_{\text{PR}}=f_{\text{balance}}\times\frac{f_{\text{out, direct}}}{f_{\text{out, direct}}+A_{\text{para}}+\dfrac{1-\eta_{\text{rad}}}{\eta_{\text{rad}}}}, \tag{3}$$

where $f_{\text{out, direct}}$ is the direct light out-coupling efficiency; $A_{\text{para}}$ is the parasitic absorption external to the perovskite layer (Cho et al., 2020).

#### 2.3.2 Management of external optical structures

External optical structures, including lenses (Shen et al., 2019; Kim et al., 2021) and microcavities (Miao et al., 2020), are useful for enhancing light outcoupling. Optimizing reflective index matching (Chen and Nurmikko, 2017; Lova et al., 2018) and employing plasmonic effects (Zhang et al., 2017) have also been demonstrated to improve $f_{\text{outcoupling}}$ for PeLEDs. Light extraction nanostructures, such as light-outcoupling hemispherical lenses have been employed to reduce waveguide and substrate modes, improving maximum EQEs of PeLEDs from 20.3% to 28.2% (Shen et al.,

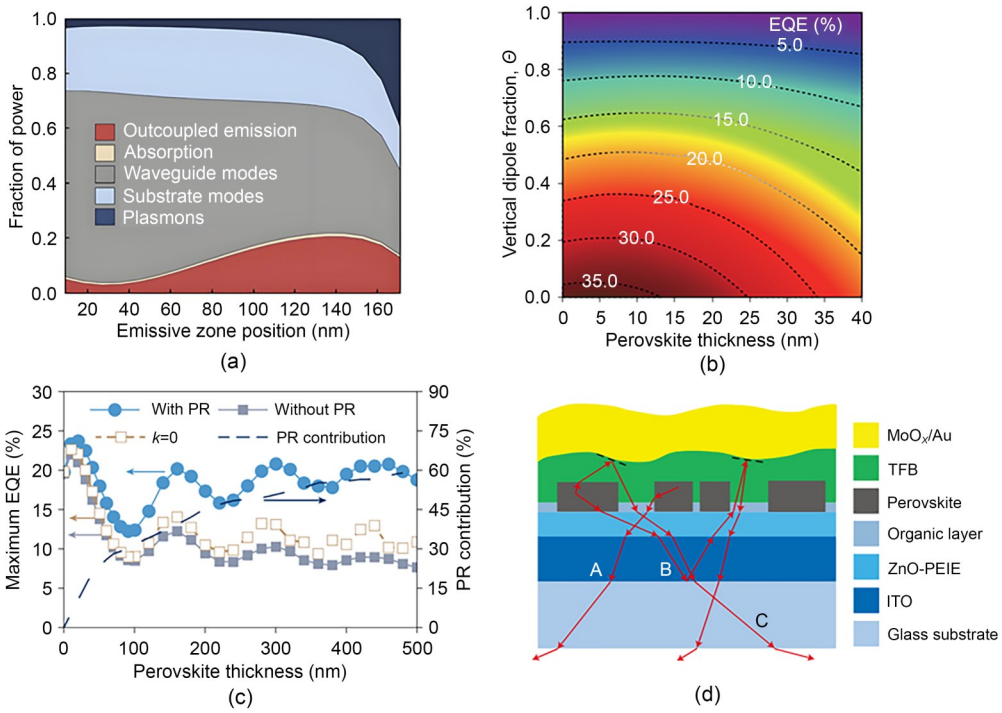


**Fig. 4 (a) Simulated fraction of power in the LED architecture as a function of emissive zone position in the PPBH emissive layer (reprinted from (Zhao et al., 2018), Copyright 2018, with permission from Springer Nature); (b) simulated EQE (color scale) as a function of $CsPbBr_3$ perovskite layer thickness and vertical dipole fraction ($\Theta$) (reprinted from (Cui et al., 2021), Copyright 2021, with permission from the American Association for the Advancement of Science; reprinted from (Zhao et al., 2023), Copyright 2023, with permission from Springer Nature); (c) simulated maximum EQE and photon recycling contribution as functions of perovskite layer thickness for a PeLED device (reprinted from (Cho et al., 2020), Copyright 2020, with permission from Springer Nature; reprinted from (Zhao et al., 2023), Copyright 2023, with permission from Springer Nature); (d) diagram of light extracted by the submicrometre structure in PeLEDs (reprinted from (Cao et al., 2018), Copyright 2018, with permission from Springer Nature). $k$ is the imaginary part of the refractive index of perovskite, and $k$=0 indicates that the perovskite is non-absorbing. PEIE is the polyethylenimine ethoxylated. References to color refer to the online version of this figure**

2019). Optical microcavities have also been employed to enhance light extraction and improve the emission properties of top-emitting PeLEDs, resulting in an increase of $f_{outcoupling}$ from about 20% to about 30%; ultimately, peak EQEs of up to 20.2% were achieved (Miao et al., 2020).

Moreover, building rough or patterned surfaces is an effective strategy to overcome the extraction limit of PeLEDs. By doping with 5-aminovaleric acid, the submicrometre structures of perovskite can efficiently improve light extraction and result in a peak EQE of 20.7%, through randomization of the paths of emitted photons (Fig. 4d) (Cao et al., 2018). Additionally, it was reported that a textured perovskite layer surface boosted the $f_{outcoupling}$ value significantly, from 11.7% to 26.5%, and the peak EQE was improved from about 10.0% to 20.5% (Chen et al., 2022).

## 3 Achieving highly stable PeLEDs

Currently, PeLEDs exhibit excellent EQEs and brightness that are comparable to (even superior to) those of OLEDs. However, the operational lifetimes ($T_{50}$, or the time for the emission intensity to decrease to 50% of the initial value) of PeLEDs are still insufficient for their commercialization (>10000 h under the required operational radiance). Here, we review the latest advances in operational stability of PeLEDs, represented by NIR, green, and blue wavelength examples, and also analyze the degradation mechanisms of PeLEDs (which are primarily related to the ionic characteristics of the perovskite lattice). The aim is to provide a reference for research into ultra-long operational lifetime PeLEDs across the entire spectrum of commercial applications.

### 3.1 State-of-the-art devices

Here we discuss recent breakthroughs in long-operational-lifetime PeLEDs with various emission wavelengths (from blue to NIR). By comparing the $T_{50}$ of PeLEDs with different colors under the same current density or irradiance, it can be found that NIR PeLEDs exhibit significantly higher operational stability than their visible counterparts (Table 1). Green, red, and blue PeLEDs have also seen encouraging progress (Kim et al., 2022; Kong et al., 2024; Dong et al., 2025), highlighting the potential for such PeLEDs in display technologies. To obtain ultra-long operational lifetimes which cannot be measured through long-term experiments, accelerated aging tests have been proposed to model the degradation of LEDs under different current densities, following this principle:

$$R_0^a \times T_{50} = C, \tag{4}$$

where $R_0$ is the initial radiance; $a$ is the acceleration factor; $C$ is a constant.

**Table 1 Summary of the stability performance of the reported PeLEDs**

| Perovskite | Structural form | Device architecture | EL peak value (nm) | Maximum EQE (%) | $T_{50}$ (h) | Test condition | Reference |
|---|---|---|---|---|---|---|---|
| SFB-10:$FAPbI_3$ | 3D | ITO/ZnO/PEIE/perovskite/TFB/$MoO_x$/Au | 803 | 22.80 | 11539 | $J$=5.00 mA/cm$^2$ | Guo et al., 2022 |
| | 3D | ITO/ZnO/PEIE/perovskite/TFB/$MoO_x$/Au | 803 | 22.80 | 32575 | $J$=3.20 mA/cm$^2$ | Guo et al., 2022 |
| | 3D | ITO/ZnO/PEIE/perovskite/TFB/$MoO_x$/Au | 803 | 22.80 | ＞3600 (no degradation) | $J$=5.00 mA/cm$^2$ | Guo et al., 2022 |
| PAC:(FA/Cs)$PbI_3$ | 3D | ITO/ZnO/PEIE/perovskite/TFB/$MoO_3$/Au | 802 | 18.60 | 682 | $J$=20.0 mA/cm$^2$ | Kuang et al., 2021 |
| MSPE:$FAPbI_3$ | 3D | ITO/ZnO/PEIE/perovskite/poly-TPD/$MoO_x$/Au | 800 | 23.80 | 32.0 | $J$=100 mA/cm$^2$ | Sun et al., 2023 |
| (Cs/Rb/FA)$PbI_3$ | 3D | ITO/ZnO/PEIE/perovskite/TFB/$MoO_3$/Au | 798 | 15.80 | 60.0 | $J$=10.0 mA/cm$^2$ | Li et al., 2020 |
| PEAI:(FA/Cs)Pb$(I/SCN)_3$ | 3D | ITO/ZnO/PEIE/perovskite/TFB/Au | 789 | 17.50 | 130 | $J$=100 mA/cm$^2$ | Guo YW et al., 2021 |
| AAs:(FA/Cs)Pb$(I/SCN)_3$ | 3D | ITO/ZnO/PEIE/perovskite/TFB/$MoO_3$/Au | 785 | 23.20 | 227 | $J$=100 mA/cm$^2$ | Li ZQ et al., 2024 |
| SFA:$FA_{0.5}Cs_{0.5}PbI_2Br$ | 3D | ITO/PEIE/ZnO/perovskite/TFB/$MoO_x$/Au | 710 | 15.40 | 357 | $J$=25.0 mA/cm$^2$ | Ren et al., 2024 |
| | 3D | ITO/PEIE/ZnO/perovskite/TFB/$MoO_x$/Au | 710 | 15.40 | 60.5 | $J$=50.0 mA/cm$^2$ | Ren et al., 2024 |
| | 3D | ITO/PEIE/ZnO/perovskite/TFB/$MoO_x$/Au | 710 | 15.40 | 21.8 | $J$=100 mA/cm$^2$ | Ren et al., 2024 |
| | 3D | ITO/PEIE/ZnO/perovskite/TFB/$MoO_x$/Au | 710 | 15.40 | 9.70 | $J$=200 mA/cm$^2$ | Ren et al., 2024 |
| | 3D | ITO/PEIE/ZnO/perovskite/TFB/$MoO_x$/Au | 710 | 15.40 | 6.30 | $J$=400 mA/cm$^2$ | Ren et al., 2024 |
| GAI:$CsPbI_3$ | 3D | ITO/$SnO_2$/a-ZnO/perovskite/TFB/$MoO_x$/Au | 703 | 18.80 | 33.6 | $J$=100 mA/cm$^2$ | Zeng et al., 2024 |
| PMA-β-$CsPbI_3$ | Nanocrystals | ITO/PEDOT:PSS/poly-TPD/perovskite/TPBi/LiF/Al | 689 | 17.80 | 317 | $J$=30.0 mA/cm$^2$ | Li et al., 2021 |
| CsPb$(Br_{0.625}/I_{0.375})_3$ | 3D | ITO/PEDOT:PSS/TFB/LiF/perovskite/TPBi/LiF/Al | 656 | 32.10 | 60.0 | $J$=5.00 mA/cm$^2$ | Feng et al., 2024 |

To be continued

Table 1 (continued)

| Perovskite | Structural form | Device architecture | EL peak value (nm) | Maximum EQE (%) | $T_{50}$ (h) | Test condition | Reference |
|---|---|---|---|---|---|---|---|
| MM-MOPA: $CsPbI_3$ | Quasi-2D | ITO/PEDOT:PSS/PTAA/PVP/perovskite/TPBi/LiF/Al | 638 | 28.70 | 127 | $J$=0.50 mA/cm$^2$ | Kong et al., 2024 |
| DPPA:$CsPb(Br/I)_3$ | Nanocrystals | ITO/PEDOT:PSS:PFI/PTAA/perovskite/TPBi/LiF/Al | 638 | 24.80 | 20.0 | $L_0$=100 cd/m$^2$ | Li HJ et al., 2024 |
| $CsPbI_3$ | QDs | ITO/PEDOT:PSS:PFI/PFN-Br/perovskite/TPBi/LiF/Al | 630 | 24.60 | 106 | $L_0$=100 cd/m$^2$ | Wei et al., 2025 |
| $MA_{0.8}FA_{0.2}PbBr_3$ | 3D | ITO/IPD/perovskite/TPBi/LiF/Al | 544 | 11.20 | 12500 | $L_0$=100 cd/m$^2$ | Chen et al., 2023 |
| BPA:$(FA_{0.7}MA_{0.1}GA_{0.2})_{0.87}Cs_{0.13}PbBr_3$ | 3D | FTO/PEDOT:PSS:PFI/perovskite/ZADN/LiF/Al | 540 | 28.90 | 31808 | $L_0$=100 cd/m$^2$ | Kim et al., 2022 |
| PEABr:$FAPbBr_3$ | Quasi-2D | FTO/$NiO_x$/PVP/perovskite/TmPPPyTz/LiF/Al | 531 | 29.50 | 50317 | $L_0$=100 cd/m$^2$ | Ding et al., 2024 |
| F-PEABr:$CsPbBr_3$ | Quasi-2D | ITO/PEDOT:PSS/PFNBr/perovskite/TmPyPB/LiF/Al | 526 | 20.36 | 0.11 | $L_0$=10000 cd/m$^2$ | Jiang et al., 2021 |
| $PEA_2Cs_{1.6}MA_{0.4}Pb_3Br_{10}$ | Quasi-2D | ITO/PEDOT:PSS/PFI/perovskite/3TPYMB/LiF/Al | 517 | 25.60 | 115 | $J$=8.00 mA/cm$^2$; $L_0$=7200 cd/m$^2$ | Ma et al., 2021 |
| Crown:MPEG-MAA:$PEA_{0.4}Cs_{0.6}PbBr_3$ | Quasi-2D | ITO/poly-TPD/LiF/perovskite/TPBi/CsF/Al | 514 | 28.10 | 4.04 | $L_0$=100 cd/m$^2$ | Liu Z et al., 2021 |
| PPNCl:p-F-PEABr:(Cs/FA/Li)$PbBr_xCl_{3-x}$ | Quasi-2D | ITO/PVP:PVK/perovskite/TPBi/Liq/Al | 474 | 13.20 | 1.12 | $L_0$=100 cd/m$^2$ | Yuan et al., 2024 |
| $CsPbBr_3$ | QDs | ITO/PEDOT:PSS/PVK/perovskite/D-ZnO/Ag | 470 | 8.70 | 35.0 | $L_0$=100 cd/m$^2$ | Liu et al., 2022 |
| $CsPbBr_3$ | QDs | ITO/PEDOT:PSS/PVK/perovskite/ZnO/Ag | 469 | 5.00 | 59.2 | $J$=7.50 mA/cm$^2$ | Yao et al., 2022 |
| $CsPbBr_3$ | QDs | ITO/PEDOT:PSS/PVK/perovskite/ZnO/Ag | 469 | 10.30 | 25.0 | $J$=12.5 mA/cm$^2$ | Bi et al., 2023 |
| F-PEA:TFA:(Cs/PBA/EA/Rb)$PbBr_xCl_{3-x}$ | Quasi-2D | ITO/SC-PEDOT/perovskite/TPBi/LiF/Al | 459 | 15.36 | 2.40 | $J$=0.45 mA/cm$^2$ | Dong et al., 2025 |
| PBA:EA:$CsPbBr_xCl_{3-x}$ | Quasi-2D | ITO/PEDOT:PSS/perovskite/TPBi/LiF/Al | 457 | 4.62 | 1.50 | $L_0$=17.2 cd/m$^2$ | Dong et al., 2022 |

PAC: pimelic acid; MSPE: 2-(4-(methylsulfonyl)phenyl)ethylamine; AAs: alkylammonium iodides; SCN: thiocyanate; SFA: sulfonamide; PMA: poly(maleic anhydride-alt-1-octadecene); MM: α-methylbenzyl-ammonium (MBA) and1-methyl-3-phenylpropyl-ammonium (MPPA); PTAA: poly[bis(4-phenyl)(2,4,6-trimethylphenyl)amine]; PVP: polyvinylpyrrolidone; PFN-Br: poly[(9,9-bis(3′-((N,N-dimethyl)-N-ethylammonium)-propyl)-2,7-fluorene)-alt-2,7(9,9-dioctylfluorene)]; ZADN: 9,10-di(naphthalene-2-yl)anthracen-2-yl-(4,1-phenylene)(1-phenyl-1H-benzo[d] imidazole); TmPPPyTz: 2,4,6-tris(3′-(pyridin-3-yl) biphenyl-3-yl)-1,3,5-triazine; TmPyPB: 1,3,5-tri(m-pyrid-3-yl-phenyl)benzene; 3TPYMB: tris[2,4,6-trimethyl-3-(pyridin-3-yl)phenyl]borane; MPEG-MAA: poly(ethylene glycol)-methyl ether acrylate; PPNCl: bis(triphenylphosphine) iminium chloride; Liq: 8-hydroxyquinolinato lithium; D-ZnO: difunctional ZnO nanocrystals; PBA: phenylbutylamine; EA: ethylamine

NIR PeLEDs have demonstrated excellent stability on par with that of OLEDs, thus meeting the demands of commercial applications. For instance, ultra-stable operation of efficient $FAPbI_3$ PeLED (Fig. 5a) (peak EQE=22.8%), with no degradation over 3600 h at 5 mA/cm$^2$, has been demonstrated (Guo et al., 2022). $T_{50}$ lifetimes of the PeLEDs, estimated by accelerated aging tests on 62 devices working under different current densities (Fig. 5b), were found to reach 32675 h (3.7 years) at an initial radiance of 2.1 W/(sr·m$^2$) (which is equivalent to green OLEDs operating at 1000 cd/m$^2$). Moreover, an ultra-long lifetime of about $2.4\times10^6$ h was projected at a lower radiance of 0.21 W/(sr·m$^2$). This breakthrough is mainly attributed to the introduction of sulfobetaine-10 (SFB-10), a dipolar molecular stabilizer that can effectively interact with ions ($FA^+$, $Pb^{2+}$, $I^-$) at grain boundaries. Ion migration and formation of lead iodide were suppressed, contributing to the stabilization of the α-phase $FAPbI_3$ perovskite. These achievements alleviated the long-held concern that PeLEDs might be inherently unstable, and demonstrated their capability for commercial applications.

Green PeLEDs have shown the highest peak EQEs among PeLEDs of all colors (Liu Z et al., 2021; Bai et al., 2023). However, their typical $T_{50}$ lifetimes were commonly several hundred hours on respective initial luminance ($L_0$) values (100–1000 cd/m$^2$), which is inferior to NIR PeLEDs operating under the same current density (Cheng et al., 2019; Zhang et al., 2020; Han et al., 2021). An advancement in the stability of green PeLEDs (Fig. 5c) resulted in a $T_{50}$ of 520 h at an $L_0$ of 1000 cd/m$^2$, and an extrapolated $T_{50}$ lifetime of 31808 h at an $L_0$ of 100 cd/m$^2$ (Fig. 5d) (Kim et al., 2022). The key to this study was the nanocrystalline structure of perovskite surrounded by a benzyl phosphonic acid shell. Benzylphosphonic acid (BPA) molecules formed covalent bonds with perovskite, which improved carrier confinement, passivated the undercoordinated lead atoms, and suppressed ion migration.

Br-I and Br-Cl mixing in perovskites is commonly used to adjust the bandgap for red and blue PeLEDs, respectively. However, red and blue PeLEDs are vulnerable to spectral shifting due to halide segregation (Vashishtha and Halpert, 2017; Yang Y et al., 2021). Sulfonamide, a dipolar molecular stabilizer, can effectively interact with the ionic species in the EMLs and suppresses halide segregation; in this way, record-high $T_{50}$ lifetimes of up to about 357 h at currents of ⩾25 mA/cm$^2$ were achieved in red PeLEDs (Ren et al., 2024). Besides, several methods to tune emission bandgaps of perovskites were proposed so as to avoid mixed-halide. For instance, through the introduction of A-site ions with a relatively small radius (such as $Rb^+$), there is contraction in the perovskite lattice, resulting in enhanced overlap between the lead and halide orbitals; this in turn, leads to a blue shift in the emission wavelength. This method successfully reduced the $Cl^-$ content in $CsPb(Br_xCl_{1-x})_3$ and further suppressed the formation of deep-level defects through $Rb^+$ compensation (Figs. 5e and 5f) (Gao et al., 2024). In addition, the reduced-dimensional perovskites (RDPs) can also adjust bandgaps without having to use mixed halides for colour tuning (Yuan et al., 2016; Lin et al., 2017). A $T_{50}$ of 7610 min at an $L_0$ of 100 cd/m$^2$ for pure-red (620–650 nm) PeLEDs has been achieved by incorporating double-end anchored ligand molecules with ammonium and methoxy groups, and methoxy-phenylethyl ammonium (MOPA) into RDP pure-iodine perovskite; a $T_{50}$ of 144 min at 0.45 mA/cm$^2$ for deep-blue (459 nm) PeLEDs was achieved by a multivalent immobilization strategy involving the introduction of a polyfluorinated oxygen-containing molecule into RDP (Fig. 5g) (Kong et al., 2024; Dong et al., 2025). Compared to NIR and green PeLEDs, achieving stable operation with red and blue PeLEDs and meeting the requirements of commercial applications (>10000 h) is even more difficult. Future research is needed to solve these issues.

Looking ahead, in addition to pursuing ultra-long lifetimes at high brightness across the full color spectrum, the poor operational stability of lead-free PeLEDs should be addressed. To facilitate the development of PeLEDs into an environmentally friendly light-source technology, Ge-, Cu-, Eu-, Bi-, and Sb-based perovskite luminescent materials have been successfully developed as potential substitutes for lead in recent research. Some key factors contributing to poor stability in lead-free perovskite devices include uncontrollable self-doping and suboptimal film formation with alternative metals (Tang et al., 2025). $Sn^{2+}$ has a propensity to be oxidized to $Sn^{4+}$ through chemical reactions (Awais et al., 2021), and these deep-level defects lead to non-radiative recombination. A targeted strategy has been presented to eliminate $Sn^{4+}$-induced defects in $CsSnI_3$-based perovskites through moisture-triggered hydrolysis of tin tetrahalide, achieving improved stability with an operational lifetime of 82.6 h (Guan et al., 2024)

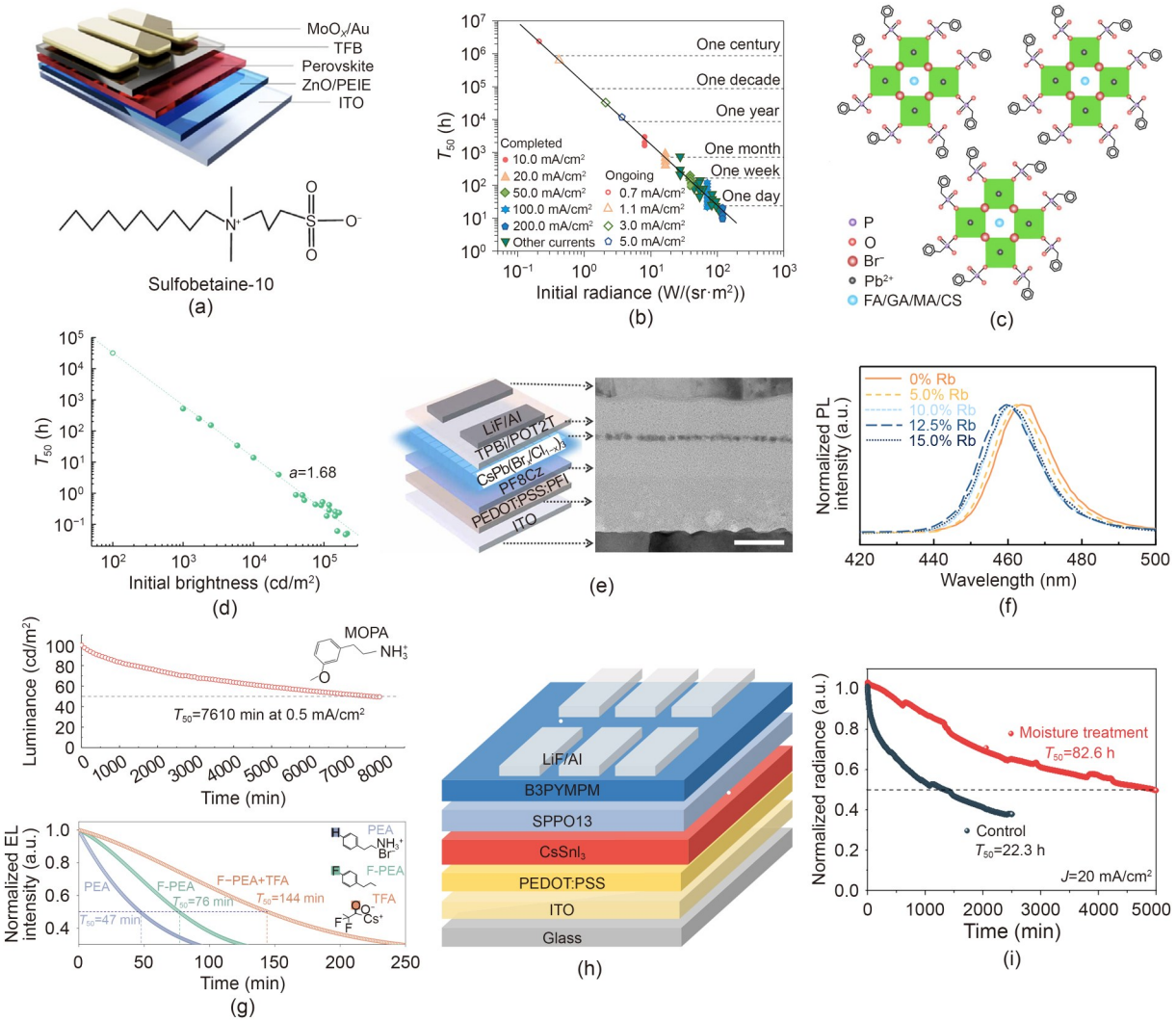


**Fig. 5 (a) Device structure of NIR PeLEDs with ultra-long lifetimes, and the molecular structure of the SFB-10 stabilizer (reprinted from (Guo et al., 2022), Copyright 2022, with permission from Springer Nature); (b) $T_{50}$ of PeLEDs stabilized with SFB-10 (reprinted from (Guo et al., 2022), Copyright 2022, with permission from Springer Nature); (c) schematic illustration of in-situ core-shell structures with perovskite nanocrystals surrounded by BPA (reprinted from (Kim et al., 2022), Copyright 2022, with permission from Springer Nature); (d) $T_{50}$ results of in-situ core-shell PeLEDs (reprinted from (Kim et al., 2022), Copyright 2022, with permission from Springer Nature); (e) schematic diagram and cross-sectional transmission electron microscope (TEM) image of the blue PeLEDs (reprinted from (Gao et al., 2024), Copyright 2024, with permission from Springer Nature); (f) tunable PL peaks of $CsPb(Br_xCl_{1-x})_3$ nanocrystals with different incorporation levels of $Rb^+$ (reprinted from (Gao et al., 2024), Copyright 2024, with permission from Springer Nature); (g) lifetimes of MOPA-treated PeLEDs at 0.5 mA/cm² (top) and lifetimes of PEA, F-PEA, and TFA at 0.45 mA/cm² (bottom) (reprinted from (Kong et al., 2024), Copyright 2024, with permission from Springer Nature; reprinted from (Dong et al., 2025), Copyright 2025, with permission from Springer Nature); (h) device structure of the $CsSnI_3$-based PeLEDs (reprinted from (Guan et al., 2024), Copyright 2024, with permission from Springer Nature); (i) lifetimes of the $CsSnI_3$-based PeLEDs with and without moisture treatment. The solid line in Fig. 5b demonstrates the fitting of lifetime data from 62 devices based on accelerated aging tests. GA and MA are the guanidine and methylamine, respectively; PF8Cz is the poly((9,9-dioctylfluorenyl-2,7-diyl)-alt-(9(2-ethylhexyl)-carbazole-3,6-diyl)); PFI is the perfluorinated resin; PL and EL are the photoluminescence and electroluminescence, respectively; PEA, F-PEA, and TFA are the phenethylamine, 4-fluorophenylethylamine, and trifluoroacetate, respectively; SPPO13 is the 2,7-bis(diphenyl phosphoryl-9,9′-spirobifluorene). References to color refer to the online version of this figure**

(Figs. 5h and 5i). To further facilitate the development of PeLEDs into an environmentally friendly light-source technology, other strategies were developed to reduce the toxicity of lead in perovskites. These include

Ge-, Cu-, Eu-, and Bi-based perovskites and double perovskites (Chung et al., 2012; Yang DX et al., 2021; Han et al., 2023; Min et al., 2023). The high oxidation potential of Ge generated a stable native oxide passivation layer on the perovskite surface, thus enhancing the stability of the $CsSn_{0.5}Ge_{0.5}I_3$ perovskite (Chen et al., 2019). Addressing the issue of poor operational stability of lead-free PeLEDs is a critical goal in the field.

### 3.2 Key mechanisms of degradation in PeLEDs

To overcome the instability of PeLEDs and meet the requirements for commercial applications, it is essential to explore the degradation mechanisms of PeLEDs. Ion migration is widely recognized as the primary cause of performance deterioration, while other contributing factors include phase transformation, halide segregation, interfacial chemical reactions, and thermal degradation.

#### 3.2.1 Ion migration

Perovskites have a soft and deformable ionic structure with mixed electronic–ionic conduction properties, which facilitate ion motion (Li et al., 2022). The movement of ionic species in perovskites depends on the activation energy required for ions to move from one equilibrium position to another. Since the activation energy for ion migration in perovskites is typically low, external stimuli such as light, bias voltage, or heat can easily trigger directional migration of ions (Li et al., 2022; Zhao et al., 2024). In addition, concentration gradients can drive the diffusive migration of ionic species. The initial observation of ion motion in perovskites, which was characterized by an abnormal dielectric response at low frequency and hysteresis in the current–voltage curve, was made in perovskite solar cells (PSCs) (Snaith et al., 2014). In comparison with PSCs, PeLEDs are vulnerable to ion migration due to the excessive amount of organic halide salts in the precursor solution and the thinner emission layer (which typically measures tens of nanometers) (Dong et al., 2020).

Ion migration in PeLEDs can be classified into two categories according to their pathways: inside EMLs, and across the interfaces (Dong et al., 2020; Liu XK et al., 2021; Woo et al., 2021). Ion migration inside EMLs can lead to defect migration and annihilation and formation of Frenkel defects, adjustment of charge injection, and distortion of the crystal lattice (Fig. 6a). Additionally, ion migration across the interfaces can result in changes in CTL properties and chemical corrosion of electrodes (Fig. 6b) (Zhao et al., 2024). These detrimental effects result in displacements of EL spectra, EQE roll-off, and luminance quenching. Aside from the dipolar molecular stabilizer method mentioned above, several strategies have been proposed to suppress ion migration, including structural and dimensional modulation, molecular passivation (Cao et al., 2018), and heat management. For example, reduced-dimensional perovskites with monodispersed quantum wells were synthesized using tris(4-fluorophenyl) phosphine oxide (TFPPO), leading to a remarkable $T_{50}$ lifetime of 115 min at $L_0$ of 7200 cd/m$^2$ (Ma et al., 2021).

#### 3.2.2 Phase transformation and halide segregation

Phase transformations under undesirable operating conditions in perovskites involve abrupt crystal lattice rearrangement or changes in symmetry, which arise from the inherent structural instability of perovskites (due to their suboptimal tolerance and octahedral structure). The index typically used to evaluate the structural stability of perovskite crystals is the Goldschmidt tolerance factor $T$, which can be calculated as (Travis et al., 2016):

$$T=\frac{r_{\mathrm{A}}+r_{\mathrm{X}}}{\sqrt{2}\,(r_{\mathrm{B}}+r_{\mathrm{X}})}, \tag{5}$$

where $r_{\mathrm{A}}$, $r_{\mathrm{B}}$, and $r_{\mathrm{X}}$ are the ionic radii of the A-site, B-site, and X-site ions, respectively. A value outside of the ideal range (which is between 0.8 and 1.0) is usually not conductive to forming a cubic perovskite structure (Jena et al., 2019). For instance, a photoactive α- phase $FAPbI_3$ perovskite is likely to degrade into a non-photoactive δ-phase at room temperature (Fig. 6c) (Fabini et al., 2016; Liu et al., 2023). Recently, low-concentration $MAPbBr_3$ (0.8% (molar fraction), $CH_3NH_3PbBr_3$; $MA^+$ corresponds to $CH_3NH_3^+$) incorporation into $FAPbI_3$ has been shown to have a beneficial effect on stabilizing the α-phase (Yoo et al., 2021).

Halide ions with low activation energy dominate ion motion in metal halide perovskites (MHPs). Halide segregation refers to the spatial compositional and structural heterogeneity that develops upon light illumination in MHPs. The formation of $Br^-$ rich and $Cl^-$ rich regions in $CsPbBr_xCl_{3-x}$ nanocrystals is due to the tendency of ion migration toward adjacent vacancy defects under bias, as well as the difference in affinity

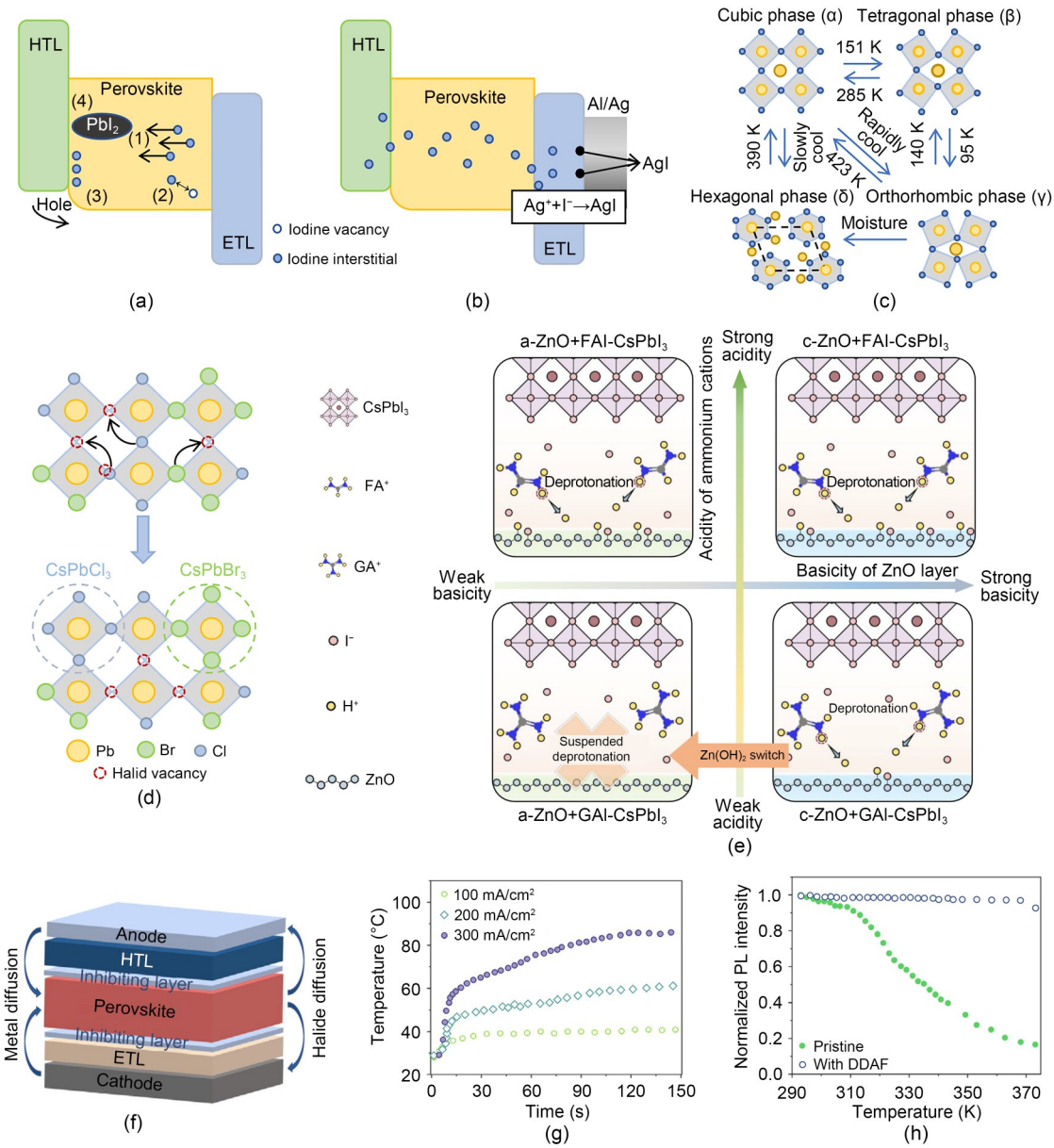


**Fig. 6 (a) Schematic diagram of ion migration effects inside perovskite on operational stability, including (1) defect migration, (2) annihilation and creation of Frenkel defects, (3) modification on charge injection, and (4) distortion of the crystal lattice (reprinted from (Dong et al., 2020), Copyright 2020, with permission from Institute of Physics Publishing); (b) electrode degradation caused by the ion migration across the interface (reprinted from (Dong et al., 2020), Copyright 2020, with permission from Institute of Physics Publishing); (c) temperature-dependent phase transition of the crystal structure of the $FAPbI_3$ absorbers (reprinted from (Liu et al., 2023), Copyright 2023, with permission from Springer Nature); (d) schematic illustration of vacancy-assisted ion migration and the resulting Br-rich and Cl-rich regions (reprinted from (Luo et al., 2020), Copyright 2020, with permission from Springer Nature); (e) schematic of interfacial deprotonation reactions based on ZnO with increased basicity and ammonium cations with increased acidities (reprinted from (Zeng et al., 2024), Copyright 2024, with permission from Springer Nature); (f) schematic illustration of inserting barrier layers to prevent device degradation, including the diffusion of metallic species from electrodes and the migration of halide ions from perovskite degradation (reprinted from (Zhao et al., 2024), Copyright 2024, with permission from Springer Nature); (g) surface temperature variations over time for a PeLED at 100, 200, and 300 $mA/cm^2$ (reprinted from (Xu et al., 2020), Copyright 2020, with permission from American Chemical Society); (h) PL intensities of pristine and DDAF-treated perovskite films at increased temperatures (reprinted from (Liu MM et al., 2021), Copyright 2021, with permission from Springer Nature). c-ZnO and a-ZnO in Fig. 6e are the colloidal ZnO and alkalescent ZnO, respectively. References to color refer to the online version of this figure**

between $Pb^{2+}$, $Br^-$, and $Cl^-$ ions, which separately facilitates the formation of $CsPbBr_3$ and $CsPbCl_3$ phases (Fig. 6d) (Luo et al., 2020). Some feasible solutions have been demonstrated to suppress halide segregation, including enhancing the barriers to halide ion migration using molecular stabilizers (Guo et al., 2022), reducing halide vacancies (Zheng et al., 2020), and vapor-assisted crystallization techniques to improve compositional homogeneity (Karlsson et al., 2021).

3.2.3 Interfacial chemical interactions

Interfacial chemical interactions occur under external bias, which is one of the main reasons for the poor stability of PeLEDs. The deprotonation of ammonium salt in organic-inorganic perovskites leads to interfacial degradation (Warby et al., 2020). For instance, $MAPbBr_3$ was reported to decompose into $PbBr_2$, $MA^+$, and $Br^-$ under electrical stress (Prakasam et al., 2019). PEABr in quasi-2D PeLEDs also undergoes a similar decomposition reaction, and is accompanied by the transformation to 3D perovskites, which further results in EL quenching (Watanabe et al., 2019).

Spontaneous interfacial chemical reactions between the EMLs and other layers may generate volatile byproducts, which can penetrate the perovskite films, leading to phase transformation or film decomposition of the perovskite EMLs (Guerrero et al., 2016; Dong et al., 2020). Unlike ion migration and electrochemical reactions, these processes do not require an external bias. The deprotonation reaction is more likely to occur with increased basicity of the metal oxide substrates and acidity of the ammonium cations (Fig. 6e), resulting in the formation of deep-level defects (Zeng et al., 2024). Typically, direct contact between ZnO ETL and $FAPbI_3$ perovskites leads to the formation of δ-$FAPbI_3$ and $PbI_2$, due to the deprotonation of the $FA^+$ cations (Yuan et al., 2019). In addition, protonation reactions may occur at the interfaces of HTLs and perovskites, as the sulfonic acid groups of PEDOT:PSS interact with halide perovskites, and further contribute to the instability of PeLEDs (Sun et al., 2021). Through surface treatment with dicarboxylic acids, which suppress deprotonation reactions between the ZnO ETL and the perovskite film, $T_{50}$ of 682 h at 20 mA/cm$^2$ for PeLEDs was achieved (Kuang et al., 2021).

In addition, metal ions in the electrodes and halide ions in the perovskite layer can infiltrate other functional layers through diffusion or migration. These ions then undergo chemical reactions with the substances in those layers, ultimately leading to device degradation. This process can be prevented through the insertion of barrier layers (Fig. 6f) (Zhao et al., 2024).

3.2.4 Thermal degradation

Joule heating, which arises from the high resistance of perovskite layers and the poor thermal conductivity of glass substrates, can initiate thermal degradation of perovskite or CTLs, leading to inferior operational stability (Kim et al., 2018; Zhao LF et al., 2019; Zhao LF et al., 2020). Perovskites containing MA tend to readily break down into MA vapor and $PbI_2$ when the temperature exceeds 85 °C (Park et al., 2023). Moreover, significant heat accumulation occurs under high current densities. When operating at 300 mA/cm$^2$, the temperature of PeLEDs can quickly exceed 80 °C within 100 s, which ultimately results in a dismal $T_{50}$ value of 3 s (Fig. 6g) (Xu et al., 2020).

Thermal management strategies can significantly improve device stability, such as employing substrates with superior thermal conductivity to glass (e.g., $SiO_2$, sapphire) (Xu et al., 2020; Zou et al., 2020), modifying surfaces to enhance the thermal conductivity of the perovskite layers (Li HJ et al., 2024), and doping CTLs (Zhao LF et al., 2020). A fluoride post-synthesis treatment with didodecyl dimethylammonium fluoride (DDAF) on PeLEDs, based on $CsPbBr_3$ nanocrystals, enabled stable and temperature-independent PL of up to 373 K with 90% PLQY. In contrast, the PLQY of the control sample declined sharply to about 15% when the temperature was increased to 370 K (Fig. 6h) (Liu MM et al., 2021).

## 4 Summary and outlook

Perovskites have emerged as promising materials for light-emitting diodes thanks to their remarkable attributes, including high color purity, high efficiency, high brightness, and tunable wavelengths. Recent breakthroughs in PeLEDs highlight their potential for applications in display and solid-state lighting. PeLEDs have demonstrated high efficiency across a range of emission wavelengths (from blue to NIR)—particularly green and red PeLEDs, which now achieve EQEs exceeding 30%. These achievements highlight the potential of PeLEDs as an alternative to OLEDs.

Such advancements have largely been driven by improvements in the optical properties of the emissive perovskite layers and the modification of device structures. We discussed the crucial factors for achieving near-unity IQEs, including enhancing effective charge injection and recombination, while suppressing nonradiative recombination losses. Additionally, employing controllable p- or n-type behaviors and charge concentration in perovskites, akin to III–V semiconductors, could further improve charge transport and enhance device performance (Xiong et al., 2024). Nevertheless, approximately 80% of the photons generated are retained within the device stack, and eventually dissipate their energy. As light outcoupling from PeLEDs improves, it may become feasible to achieve EQEs approaching 100%. Such an advancement could pave the way for low-cost ultra-high-performance light sources (Zhao et al., 2023).

Recent advances in the operational stability of PeLEDs with NIR and green emission wavelengths suggest that PeLEDs are transitioning from a laboratory curiosity to a commercially viable technology (Guo et al., 2022; Kim et al., 2022). To achieve long-term operational stability across the full color spectrum, future studies could concentrate on molecular stabilizers that mitigate the effects of ion migration and halide segregation, investigate suppression of chemical interactions at interfaces between perovskite grain boundaries and functional layers, and improve thermal management. Moreover, developing novel structure designs such as core-shell nanocrystals and heterostructures, along with effective interfacial layers and modifications, may further enhance the stability of PeLEDs. Furthermore, inorganic CTLs, which have played a key role in the exceptional stability of novel NIR PeLEDs, could be explored for further use in PeLEDs of different color ranges (Zhao et al., 2024).

Despite encouraging breakthroughs in PeLEDs, several issues must still be overcome. First off, high-performance standard blue PeLEDs (peak wavelengths ⩽470 nm) are a rarity. Their EQEs are normally less than 15% with poor operational stability (Wang CH et al., 2020; Zhou et al., 2022), restricting application in wide-color-gamut displays. Future research should focus on understanding nucleation, crystallization, nonradiative losses, and the aging mechanisms of blue perovskite emitters in order to improve their efficiency and stability. Sn-based PeLEDs, which are not toxic, stand out as the most promising alternative to lead-based perovskites. However, the operational stability of Sn-based PeLEDs (which is currently limited to tens of hours) is severely lacking compared to their lead-based counterparts (Tang et al., 2025). The realization of high-performance lead-free perovskites, therefore remains a critical research gap. Mitigating the toxicity of PeLEDs would pave the way for more successful commercial applications.

In addition, the long lifetimes under low brightness for PeLEDs, which are estimated by accelerated aging methods with data collected from short-term experiments, typically deviate from the true values. Methods that can obtain accurate long-term lifetime operation data need to be explored further, so as to offer an in-depth understanding of degradation mechanisms and promote operational stability of PeLEDs. Lastly, improving device performance under high-brightness operation remains a significant challenge for PeLEDs, which has thus far restricted their application in holographic imaging, lighting, and electrically pumped lasing. To increase the peak brightness and improve device stability under high current densities, key factors such as Auger recombination, charge transport, and Joule heating must be addressed.

Looking forward, we anticipate that significant challenges in PeLEDs, such as the limited performance of blue and lead-free devices, and the instability of visible PeLEDs, will be resolved. As such, the potential of this technology will be realized, and more stable and efficient PeLEDs may be developed.

## Acknowledgments

This work is supported by the National Key Research and Development Program of China (No. 2022YFA1204800), the Scientific Research Innovation Capability Support Project for Young Faculty (No. ZYGXQNJSKYCXNLZCXM-I25), China, the National Natural Science Foundation of China (No. 62274144), and the Zhejiang Provincial Government, China.

## Author contributions

Zhuoyue GU drafted the outline of the review paper under the guidance of Dawei DI; Zhuoyue GU and Suhui ZHANG wrote the initial draft of the manuscript, which was revised by Dawei DI, Baodan ZHAO, and Wentao XIONG.

## Conflict of interest

Zhuoyue GU, Suhui ZHANG, Wentao XIONG, Baodan ZHAO, and Dawei DI declare that they have no conflict of interest.

## References


Awais M, Kirsch RL, Yeddu V, et al., 2021. Tin halide perovskites going forward: frost diagrams offer hints. *ACS Materials Letters*, 3(3):299-307. https://doi.org/10.1021/acsmaterialslett.0c00571

Bai WH, Xuan TT, Zhao HY, et al., 2023. Perovskite light-emitting diodes with an external quantum efficiency exceeding 30%. *Advanced Materials*, 35(39):2302283. https://doi.org/10.1002/adma.202302283

Ball JM, Petrozza A, 2016. Defects in perovskite-halides and their effects in solar cells. *Nature Energy*, 1(11):16149. https://doi.org/10.1038/nenergy.2016.149

Ban MY, Zou YT, Rivett JPH, et al., 2018. Solution-processed perovskite light emitting diodes with efficiency exceeding 15% through additive-controlled nanostructure tailoring. *Nature Communications*, 9(1):3892. https://doi.org/10.1038/s41467-018-06425-5

Bi CH, Yao ZW, Hu JC, et al., 2023. Suppressing Auger recombination of perovskite quantum dots for efficient pure-blue-light-emitting diodes. *ACS Energy Letters*, 8(1):731-739. https://doi.org/10.1021/acsenergylett.2c02613

Bowman AR, Anaya M, Greenham NC, et al., 2020. Quantifying photon recycling in solar cells and light-emitting diodes: absorption and emission are always key. *Physical Review Letters*, 125(6):067401. https://doi.org/10.1103/PhysRevLett.125.067401

Cao Y, Wang NN, Tian H, et al., 2018. Perovskite light-emitting diodes based on spontaneously formed submicrometre-scale structures. *Nature*, 562(7726):249-253. https://doi.org/10.1038/s41586-018-0576-2

Chen B, Rudd PN, Yang S, et al., 2019. Imperfections and their passivation in halide perovskite solar cells. *Chemical Society Reviews*, 48(14):3842-3867. https://doi.org/10.1039/C8CS00853A

Chen J, Ma PC, Chen WJ, et al., 2021. Overcoming outcoupling limit in perovskite light-emitting diodes with enhanced photon recycling. *Nano Letters*, 21(19):8426-8432. https://doi.org/10.1021/acs.nanolett.1c03035

Chen ST, Nurmikko A, 2017. Stable green perovskite vertical-cavity surface-emitting lasers on rigid and flexible substrates. *ACS Photonics*, 4(10):2486-2494. https://doi.org/10.1021/acsphotonics.7b00713

Chen WJ, Chen J, Gu LH, et al., 2022. Overcoming the outcoupling limit of perovskite light-emitting diodes with artificially formed nanostructures. *Advanced Materials*, 34(49):2207180. https://doi.org/10.1002/adma.202207180

Chen WJ, Huang ZM, Yao HT, et al., 2023. Highly bright and stable single-crystal perovskite light-emitting diodes. *Nature Photonics*, 17(5):401-407. https://doi.org/10.1038/s41566-023-01167-3

Chen ZM, Li ZC, Hopper TR, et al., 2021. Materials, photophysics and device engineering of perovskite light-emitting diodes. *Reports on Progress in Physics*, 84(4):046401. https://doi.org/10.1088/1361-6633/abefba

Cheng L, Jiang T, Cao Y, et al., 2020. Multiple-quantum-well perovskites for high-performance light-emitting diodes. *Advanced Materials*, 32(15):1904163. https://doi.org/10.1002/adma.201904163

Cheng LP, Huang JS, Shen Y, et al., 2019. Efficient $CsPbBr_3$ perovskite light-emitting diodes enabled by synergetic morphology control. *Advanced Optical Materials*, 7(4):1801534. https://doi.org/10.1002/adom.201801534

Cho C, Greenham NC, 2021. Computational study of dipole radiation in re-absorbing perovskite semiconductors for optoelectronics. *Advanced Science*, 8(4):2003559. https://doi.org/10.1002/advs.202003559

Cho C, Zhao BD, Tainter GD, et al., 2020. The role of photon recycling in perovskite light-emitting diodes. *Nature Communications*, 11(1):611. https://doi.org/10.1038/s41467-020-14401-1

Cho H, Jeong SH, Park MH, et al., 2015. Overcoming the electroluminescence efficiency limitations of perovskite light-emitting diodes. *Science*, 350(6265):1222-1225. https://doi.org/10.1126/science.aad1818

Chung I, Song J, Im J, et al., 2012. $CsSnI_3$: semiconductor or metal? High electrical conductivity and strong near-infrared photoluminescence from a single material. High hole mobility and phase-transitions. *Journal of the American Chemical Society*, 134(20):8579-8587. https://doi.org/10.1021/ja301539s

Cui JY, Liu Y, Deng YZ, et al., 2021. Efficient light-emitting diodes based on oriented perovskite nanoplatelets. *Science Advances*, 7(41):eabg8458. https://doi.org/10.1126/sciadv.abg8458

Ding S, Wang QQ, Gu WC, et al., 2024. Phase dimensions resolving of efficient and stable perovskite light-emitting diodes at high brightness. *Nature Photonics*, 18(4):363-370. https://doi.org/10.1038/s41566-023-01372-0

Dong JC, Lu FF, Han DY, et al., 2022. Deep-blue electroluminescence of perovskites with reduced dimensionality achieved by manipulating adsorption-energy differences. *Angewandte Chemie International Edition*, 61(40):e202210322. https://doi.org/10.1002/anie.202210322

Dong JC, Zhao B, Ji HY, et al., 2025. Multivalent-effect immobilization of reduced-dimensional perovskites for efficient and spectrally stable deep-blue light-emitting diodes. *Nature Nanotechnology*, 20(4):507-514. https://doi.org/10.1038/s41565-024-01852-6

Dong Q, Lei L, Mendes J, et al., 2020. Operational stability of perovskite light emitting diodes. *Journal of Physics: Materials*, 3(1):012002. https://doi.org/10.1088/2515-7639/ab60c4

Fabini DH, Stoumpos CC, Laurita G, et al., 2016. Reentrant structural and optical properties and large positive thermal expansion in perovskite formamidinium lead iodide. *Angewandte Chemie International Edition*, 55(49):15392-15396. https://doi.org/10.1002/anie.201609538

Fakharuddin A, Qiu WM, Croes G, et al., 2019. Reduced efficiency roll-off and improved stability of mixed 2D/3D perovskite light emitting diodes by balancing charge injection. *Advanced Functional Materials*, 29(37):1904101.

https://doi.org/10.1002/adfm.201904101

Fakharuddin A, Gangishetty MK, Abdi-Jalebi M, et al., 2022. Perovskite light-emitting diodes. *Nature Electronics*, 5(4): 203-216. https://doi.org/10.1038/s41928-022-00745-7

Feng SC, Shen Y, Hu XM, et al., 2024. Efficient and stable red perovskite light-emitting diodes via thermodynamic crystallization control. *Advanced Materials*, 36(44):2410255. https://doi.org/10.1002/adma.202410255

Fieramosca A, de Marco L, Passoni M, et al., 2018. Tunable out-of-plane excitons in 2D single-crystal perovskites. *ACS Photonics*, 5(10):4179-4185. https://doi.org/10.1021/acsphotonics.8b00984

Gao Y, Cai QT, He YF, et al., 2024. Highly efficient blue light-emitting diodes based on mixed-halide perovskites with reduced chlorine defects. *Science Advances*, 10(29): eado5645. https://doi.org/10.1126/sciadv.ado5645

Guan X, Li YQ, Meng YY, et al., 2024. Targeted elimination of tetravalent-Sn-induced defects for enhanced efficiency and stability in lead-free NIR-II perovskite LEDs. *Nature Communications*, 15(1):9913. https://doi.org/10.1038/s41467-024-54160-x

Guerrero A, You JB, Aranda C, et al., 2016. Interfacial degradation of planar lead halide perovskite solar cells. *ACS Nano*, 10(1):218-224. https://doi.org/10.1021/acsnano.5b03687

Guo BB, Lai RC, Jiang SJ, et al., 2022. Ultrastable near-infrared perovskite light-emitting diodes. *Nature Photonics*, 16(9): 637-643. https://doi.org/10.1038/s41566-022-01046-3

Guo YW, Apergi S, Li N, et al., 2021. Phenylalkylammonium passivation enables perovskite light emitting diodes with record high-radiance operational lifetime: the chain length matters. *Nature Communications*, 12(1):644. https://doi.org/10.1038/s41467-021-20970-6

Guo ZY, Zhang Y, Wang BZ, et al., 2021. Promoting energy transfer via manipulation of crystallization kinetics of quasi-2D perovskites for efficient green light-emitting diodes. *Advanced Materials*, 33(40):2102246. https://doi.org/10.1002/adma.202102246

Han BN, Yuan SC, Cai B, et al., 2021. Green perovskite light-emitting diodes with 200 hours stability and 16% efficiency: cross-linking strategy and mechanism. *Advanced Functional Materials*, 31(26):2011003. https://doi.org/10.1002/adfm.202011003

Han DY, Wang J, Agosta L, et al., 2023. Tautomeric mixture coordination enables efficient lead-free perovskite LEDs. *Nature*, 622(7983):493-498. https://doi.org/10.1038/s41586-023-06514-6

Hassan Y, Park JH, Crawford ML, et al., 2021. Ligand-engineered bandgap stability in mixed-halide perovskite LEDs. *Nature*, 591(7848):72-77. https://doi.org/10.1038/s41586-021-03217-8

Jena AK, Kulkarni A, Miyasaka T, 2019. Halide perovskite photovoltaics: background, status, and future prospects. *Chemical Reviews*, 119(5):3036-3103. https://doi.org/10.1021/acs.chemrev.8b00539

Jiang YZ, Cui MH, Li SS, et al., 2021. Reducing the impact of Auger recombination in quasi-2D perovskite light-emitting diodes. *Nature Communications*, 12(1):336. https://doi.org/10.1038/s41467-020-20555-9

Karlsson M, Yi ZY, Reichert S, et al., 2021. Mixed halide perovskites for spectrally stable and high-efficiency blue light-emitting diodes. *Nature Communications*, 12(1):361. https://doi.org/10.1038/s41467-020-20582-6

Kim H, Zhao LF, Price JS, et al., 2018. Hybrid perovskite light emitting diodes under intense electrical excitation. *Nature Communications*, 9(1):4893. https://doi.org/10.1038/s41467-018-07383-8

Kim JS, Heo JM, Park GS, et al., 2022. Ultra-bright, efficient and stable perovskite light-emitting diodes. *Nature*, 611(7937): 688-694. https://doi.org/10.1038/s41586-022-05304-w

Kim YH, Kim S, Kakekhani A, et al., 2021. Comprehensive defect suppression in perovskite nanocrystals for high-efficiency light-emitting diodes. *Nature Photonics*, 15(2): 148-155. https://doi.org/10.1038/s41566-020-00732-4

Kong LM, Sun YQ, Zhao B, et al., 2024. Fabrication of red-emitting perovskite LEDs by stabilizing their octahedral structure. *Nature*, 631(8019):73-79. https://doi.org/10.1038/s41586-024-07531-9

Kuang CY, Hu ZJ, Yuan ZC, et al., 2021. Critical role of additive-induced molecular interaction on the operational stability of perovskite light-emitting diodes. *Joule*, 5(3):618-630. https://doi.org/10.1016/j.joule.2021.01.003

Lee S, Park JH, Nam YS, et al., 2018. Growth of nanosized single crystals for efficient perovskite light-emitting diodes. *ACS Nano*, 12(4):3417-3423. https://doi.org/10.1021/acsnano.7b09148

Lee S, Kim DB, Yu JC, et al., 2019. Versatile defect passivation methods for metal halide perovskite materials and their application to light-emitting devices. *Advanced Materials*, 31(20):1805244. https://doi.org/10.1002/adma.201805244

Li HJ, Zhu XF, Zhang DS, et al., 2024. Thermal management towards ultra-bright and stable perovskite nanocrystal-based pure red light-emitting diodes. *Nature Communications*, 15(1):6561. https://doi.org/10.1038/s41467-024-50634-0

Li HM, Lin H, Ouyang D, et al., 2021. Efficient and stable red perovskite light-emitting diodes with operational stability >300 h. *Advanced Materials*, 33(15):2008820. https://doi.org/10.1002/adma.202008820

Li MM, Yang YG, Kuang ZY, et al., 2024. Acceleration of radiative recombination for efficient perovskite LEDs. *Nature*, 630(8017):631-635. https://doi.org/10.1038/s41586-024-07460-7

Li N, Song L, Jia YH, et al., 2020. Stabilizing perovskite light-emitting diodes by incorporation of binary alkali cations. *Advanced Materials*, 32(17):1907786. https://doi.org/10.1002/adma.201907786

Li N, Jia YH, Guo YW, et al., 2022. Ion migration in perovskite light-emitting diodes: mechanism, characterizations, and material and device engineering. *Advanced Materials*,

34(19):2108102.
https://doi.org/10.1002/adma.202108102

Li YQ, Guan X, Zhao YP, et al., 2025. Modulation of charge transport layer for perovskite light-emitting diodes. *Advanced Materials*, 37(25):2410535.
https://doi.org/10.1002/adma.202410535

Li ZQ, Ren ZW, Liang Q, et al., 2024. Grain orientation management and recombination suppression for ultra-stable PeLEDs with record brightness. *Joule*, 8(4):1176-1190.
https://doi.org/10.1016/j.joule.2024.03.004

Lin KB, Xing J, Quan LN, et al., 2018. Perovskite light-emitting diodes with external quantum efficiency exceeding 20 per cent. *Nature*, 562(7726):245-248.
https://doi.org/10.1038/s41586-018-0575-3

Lin Y, Bai Y, Fang YJ, et al., 2017. Suppressed ion migration in low-dimensional perovskites. *ACS Energy Letters*, 2(7):1571-1572.
https://doi.org/10.1021/acsenergylett.7b00442

Liu AQ, Bi CH, Tian JJ, 2022. All solution-processed high performance pure-blue perovskite quantum-dot light-emitting diodes. *Advanced Functional Materials*, 32(44):2207069.
https://doi.org/10.1002/adfm.202207069

Liu MM, Wan Q, Wang HM, et al., 2021. Suppression of temperature quenching in perovskite nanocrystals for efficient and thermally stable light-emitting diodes. *Nature Photonics*, 15(5):379-385.
https://doi.org/10.1038/s41566-021-00766-2

Liu XK, Xu WD, Bai S, et al., 2021. Metal halide perovskites for light-emitting diodes. *Nature Materials*, 20(1):10-21.
https://doi.org/10.1038/s41563-020-0784-7

Liu XP, Luo DY, Lu ZH, et al., 2023. Stabilization of photoactive phases for perovskite photovoltaics. *Nature Reviews Chemistry*, 7(7):462-479.
https://doi.org/10.1038/s41570-023-00492-z

Liu Z, Qiu WD, Peng XM, et al., 2021. Perovskite light-emitting diodes with EQE exceeding 28% through a synergetic dual-additive strategy for defect passivation and nanostructure regulation. *Advanced Materials*, 33(43):2103268.
https://doi.org/10.1002/adma.202103268

Lova P, Cortecchia D, Krishnamoorthy HNS, et al., 2018. Engineering the emission of broadband 2D perovskites by polymer distributed Bragg reflectors. *ACS Photonics*, 5(3):867-874.
https://doi.org/10.1021/acsphotonics.7b01077

Luo C, Yan C, Li W, et al., 2020. Ultrafast thermodynamic control for stable and efficient mixed halide perovskite nanocrystals. *Advanced Functional Materials*, 30(19):2000026.
https://doi.org/10.1002/adfm.202000026

Luo DY, Su R, Zhang W, et al., 2019. Minimizing non-radiative recombination losses in perovskite solar cells. *Nature Reviews Materials*, 5(1):44-60.
https://doi.org/10.1038/s41578-019-0151-y

Luo Y, Kong LM, Wang L, et al., 2022. A multifunctional ionic liquid additive enabling stable and efficient perovskite light-emitting diodes. *Small*, 18(19):2200498.
https://doi.org/10.1002/smll.202200498

Ma DX, Lin KB, Dong YT, et al., 2021. Distribution control enables efficient reduced-dimensional perovskite LEDs. *Nature*, 599(7886):594-598.
https://doi.org/10.1038/s41586-021-03997-z

Miao YF, Cheng L, Zou W, et al., 2020. Microcavity top-emission perovskite light-emitting diodes. *Light: Science & Applications*, 9(1):89.
https://doi.org/10.1038/s41377-020-0328-6

Min H, Chang J, Tong YF, et al., 2023. Additive treatment yields high-performance lead-free perovskite light-emitting diodes. *Nature Photonics*, 17(9):755-760.
https://doi.org/10.1038/s41566-023-01231-y

Nenon DP, Pressler K, Kang J, et al., 2018. Design principles for trap-free $CsPbX_3$ nanocrystals: enumerating and eliminating surface halide vacancies with softer Lewis bases. *Journal of the American Chemical Society*, 140(50):17760-17772.
https://doi.org/10.1021/jacs.8b11035

Park J, Kim J, Yun HS, et al., 2023. Controlled growth of perovskite layers with volatile alkylammonium chlorides. *Nature*, 616(7958):724-730.
https://doi.org/10.1038/s41586-023-05825-y

Prakasam V, Tordera D, Bolink HJ, et al., 2019. Degradation mechanisms in organic lead halide perovskite light-emitting diodes. *Advanced Optical Materials*, 7(22):1900902.
https://doi.org/10.1002/adom.201900902

Proppe AH, Walters GW, Alsalloum AY, et al., 2020. Transition dipole moments of $n$=1, 2, and 3 perovskite quantum wells from the optical stark effect and many-body perturbation theory. *The Journal of Physical Chemistry Letters*, 11(3):716-723.
https://doi.org/10.1021/acs.jpclett.9b03349

Quan LN, Zhao YB, García de Arquer FP, et al., 2017. Tailoring the energy landscape in quasi-2D halide perovskites enables efficient green-light emission. *Nano Letters*, 17(6):3701-3709.
https://doi.org/10.1021/acs.nanolett.7b00976

Quan LN, Ma DX, Zhao YB, et al., 2020. Edge stabilization in reduced-dimensional perovskites. *Nature Communications*, 11(1):170.
https://doi.org/10.1038/s41467-019-13944-2

Ren ZW, Yu JH, Qin ZT, et al., 2021. High-performance blue perovskite light-emitting diodes enabled by efficient energy transfer between coupled quasi-2D perovskite layers. *Advanced Materials*, 33(1):2005570.
https://doi.org/10.1002/adma.202005570

Ren ZX, Guo BB, Liu SN, et al., 2024. Bright and stable red perovskite LEDs under high current densities. *ACS Applied Materials & Interfaces*, 16(7):9012-9019.
https://doi.org/10.1021/acsami.3c16922

Richter JM, Abdi-Jalebi M, Sadhanala A, et al., 2016. Enhancing photoluminescence yields in lead halide perovskites by photon recycling and light out-coupling. *Nature Communications*, 7(1):13941.
https://doi.org/10.1038/ncomms13941

Shen XY, Kang K, Yu ZK, et al., 2023. Passivation strategies for mitigating defect challenges in halide perovskite light-emitting diodes. *Joule*, 7(2):272-308.
https://doi.org/10.1016/j.joule.2023.01.008

Shen Y, Cheng LP, Li YQ, et al., 2019. High-efficiency

perovskite light-emitting diodes with synergetic outcoupling enhancement. *Advanced Materials*, 31(24):1901517. https://doi.org/10.1002/adma.201901517

Si JJ, Liu Y, He ZF, et al., 2017. Efficient and high-color-purity light-emitting diodes based on in situ grown films of $CsPbX_3$ (X=Br, I) nanoplates with controlled thicknesses. *ACS Nano*, 11(11):11100-11107. https://doi.org/10.1021/acsnano.7b05191

Snaith HJ, Abate A, Ball JM, et al., 2014. Anomalous hysteresis in perovskite solar cells. *The Journal of Physical Chemistry Letters*, 5(9):1511-1515. https://doi.org/10.1021/jz500113x

Stranks SD, Hoye RLZ, Di DW, et al., 2019. The physics of light emission in halide perovskite devices. *Advanced Materials*, 31(47):1803336. https://doi.org/10.1002/adma.201803336

Sun CJ, Jiang YZ, Cui MH, et al., 2021. High-performance large-area quasi-2D perovskite light-emitting diodes. *Nature Communications*, 12(1):2207. https://doi.org/10.1038/s41467-021-22529-x

Sun SQ, Tai JW, He W, et al., 2024. Enhancing light outcoupling efficiency via anisotropic low refractive index electron transporting materials for efficient perovskite light-emitting diodes. *Advanced Materials*, 36(24):2400421. https://doi.org/10.1002/adma.202400421

Sun YQ, Ge LS, Dai LJ, et al., 2023. Bright and stable perovskite light-emitting diodes in the near-infrared range. *Nature*, 615(7954):830-835. https://doi.org/10.1038/s41586-023-05792-4

Tan ZK, Moghaddam RS, Lai ML, et al., 2014. Bright light-emitting diodes based on organometal halide perovskite. *Nature Nanotechnology*, 9(9):687-692. https://doi.org/10.1038/nnano.2014.149

Tang WD, Liu SN, Zhang G, et al., 2025. Lead-free perovskite light-emitting diodes. *Advanced Materials*, 37(25):2411020. https://doi.org/10.1002/adma.202411020

Travis W, Glover ENK, Bronstein H, et al., 2016. On the application of the tolerance factor to inorganic and hybrid halide perovskites: a revised system. *Chemical Science*, 7(7):4548-4556. https://doi.org/10.1039/C5SC04845A

Vashishtha P, Halpert JE, 2017. Field-driven ion migration and color instability in red-emitting mixed halide perovskite nanocrystal light-emitting diodes. *Chemistry of Materials*, 29(14):5965-5973. https://doi.org/10.1021/acs.chemmater.7b01609

Wang CH, Han DB, Wang JH, et al., 2020. Dimension control of in situ fabricated $CsPbClBr_2$ nanocrystal films toward efficient blue light-emitting diodes. *Nature Communications*, 11(1):6428. https://doi.org/10.1038/s41467-020-20163-7

Wang HR, Gong XW, Zhao DW, et al., 2020. A multi-functional molecular modifier enabling efficient large-area perovskite light-emitting diodes. *Joule*, 4(9):1977-1987. https://doi.org/10.1016/j.joule.2020.07.002

Wang L, Xiao L, Gu HS, et al., 2019. Advances in alternating current electroluminescent devices. *Advanced Optical Materials*, 7(7):1801154. https://doi.org/10.1002/adom.201801154

Wang NN, Cheng L, Ge R, et al., 2016. Perovskite light-emitting diodes based on solution-processed self-organized multiple quantum wells. *Nature Photonics*, 10(11):699-704. https://doi.org/10.1038/nphoton.2016.185

Warby JH, Wenger B, Ramadan AJ, et al., 2020. Revealing factors influencing the operational stability of perovskite light-emitting diodes. *ACS Nano*, 14(7):8855-8865. https://doi.org/10.1021/acsnano.0c03516

Watanabe S, Cheng T, Tumen-Ulzii G, et al., 2019. Excited-state stability of quasi-two-dimensional metal halide perovskite films under optical and electrical excitations. *Applied Physics Letters*, 115(23):233502. https://doi.org/10.1063/1.5127308

Wei KY, Zhou T, Jiang YZ, et al., 2025. Perovskite heteroepitaxy for high-efficiency and stable pure-red LEDs. *Nature*, 638(8052):949-956. https://doi.org/10.1038/s41586-024-08503-9

Woo SJ, Kim JS, Lee TW, 2021. Characterization of stability and challenges to improve lifetime in perovskite LEDs. *Nature Photonics*, 15(9):630-634. https://doi.org/10.1038/s41566-021-00863-2

Xiao ZG, Kerner RA, Zhao LF, et al., 2017. Efficient perovskite light-emitting diodes featuring nanometre-sized crystallites. *Nature Photonics*, 11(2):108-115. https://doi.org/10.1038/nphoton.2016.269

Xing GC, Wu B, Wu XY, et al., 2017. Transcending the slow bimolecular recombination in lead-halide perovskites for electroluminescence. *Nature Communications*, 8(1):14558. https://doi.org/10.1038/ncomms14558

Xiong WT, Zou C, Tang WD, et al., 2023. Efficient and bright blue perovskite LEDs enabled by a carbazole-phosphonic acid interface. *ACS Energy Letters*, 8(7):2897-2903. https://doi.org/10.1021/acsenergylett.3c00589

Xiong WT, Tang WD, Zhang G, et al., 2024. Controllable p- and n-type behaviours in emissive perovskite semiconductors. *Nature*, 633(8029):344-350. https://doi.org/10.1038/s41586-024-07792-4

Xu H, Wang XC, Li Y, et al., 2020. Prominent heat dissipation in perovskite light-emitting diodes with reduced efficiency droop for silicon-based display. *The Journal of Physical Chemistry Letters*, 11(9):3689-3698. https://doi.org/10.1021/acs.jpclett.0c00792

Xu WD, Hu Q, Bai S, et al., 2019. Rational molecular passivation for high-performance perovskite light-emitting diodes. *Nature Photonics*, 13(6):418-424. https://doi.org/10.1038/s41566-019-0390-x

Yang DX, Zhang GL, Lai RC, et al., 2021. Germanium-lead perovskite light-emitting diodes. *Nature Communications*, 12(1):4295. https://doi.org/10.1038/s41467-021-24616-5

Yang Y, Xu S, Ni ZY, et al., 2021. Highly efficient pure-blue light-emitting diodes based on rubidium and chlorine alloyed metal halide perovskite. *Advanced Materials*, 33(33):2100783. https://doi.org/10.1002/adma.202100783

Yao ZW, Bi CH, Liu AQ, et al., 2022. High brightness and stability pure-blue perovskite light-emitting diodes based

on a novel structural quantum-dot film. *Nano Energy*, 95: 106974.
https://doi.org/10.1016/j.nanoen.2022.106974

Yoo JJ, Seo G, Chua MR, et al., 2021. Efficient perovskite solar cells via improved carrier management. *Nature*, 590(7847): 587-593.
https://doi.org/10.1038/s41586-021-03285-w

Yu ZK, Jeong WH, Kang K, et al., 2022. A polymer/small-molecule binary-blend hole transport layer for enhancing charge balance in blue perovskite light emitting diodes. *Journal of Materials Chemistry A*, 10(26):13928-13935.
https://doi.org/10.1039/D2TA01987F

Yuan MJ, Quan LN, Comin R, et al., 2016. Perovskite energy funnels for efficient light-emitting diodes. *Nature Nanotechnology*, 11(10):872-877.
https://doi.org/10.1038/nnano.2016.110

Yuan S, Dai LJ, Sun YQ, et al., 2024. Efficient blue electroluminescence from reduced-dimensional perovskites. *Nature Photonics*, 18(5):425-431.
https://doi.org/10.1038/s41566-024-01382-6

Yuan ZC, Miao YF, Hu ZJ, et al., 2019. Unveiling the synergistic effect of precursor stoichiometry and interfacial reactions for perovskite light-emitting diodes. *Nature Communications*, 10(1):2818.
https://doi.org/10.1038/s41467-019-10612-3

Zeng JJ, Sun XY, Liu Y, et al., 2024. Switchable interfacial reaction enables bright and stable deep-red perovskite light-emitting diodes. *Nature Photonics*, 18(4):325-333.
https://doi.org/10.1038/s41566-023-01369-9

Zhang L, Yuan F, Xi J, et al., 2020. Suppressing ion migration enables stable perovskite light-emitting diodes with all-inorganic strategy. *Advanced Functional Materials*, 30(40): 2001834.
https://doi.org/10.1002/adfm.202001834

Zhang Q, Song YH, Hao JM, et al., 2022. α-$BaF_2$ nanoparticle substrate-enabled γ-$CsPbI_3$ heteroepitaxial growth for efficient and bright deep-red light-emitting diodes. *Journal of the American Chemical Society*, 144(18):8162-8170.
https://doi.org/10.1021/jacs.2c01034

Zhang XL, Xu B, Wang WG, et al., 2017. Plasmonic perovskite light-emitting diodes based on the Ag–$CsPbBr_3$ system. *ACS Applied Materials & Interfaces*, 9(5):4926-4931.
https://doi.org/10.1021/acsami.6b12450

Zhao BD, Bai S, Kim V, et al., 2018. High-efficiency perovskite–polymer bulk heterostructure light-emitting diodes. *Nature Photonics*, 12(12):783-789.
https://doi.org/10.1038/s41566-018-0283-4

Zhao BD, Lian YX, Cui LS, et al., 2020. Efficient light-emitting diodes from mixed-dimensional perovskites on a fluoride interface. *Nature Electronics*, 3(11):704-710.
https://doi.org/10.1038/s41928-020-00487-4

Zhao BD, Vasilopoulou M, Fakharuddin A, et al., 2023. Light management for perovskite light-emitting diodes. *Nature Nanotechnology*, 18(9):981-992.
https://doi.org/10.1038/s41565-023-01482-4

Zhao BD, Guo BB, Xing SY, et al., 2024. Highly stable perovskite light-emitting diodes. *Matter*, 7(3):772-793.
https://doi.org/10.1016/j.matt.2023.11.022

Zhao LF, Lee KM, Roh K, et al., 2019. Improved outcoupling efficiency and stability of perovskite light-emitting diodes using thin emitting layers. *Advanced Materials*, 31(2): 1805836.
https://doi.org/10.1002/adma.201805836

Zhao LF, Roh K, Kacmoli S, et al., 2020. Thermal management enables bright and stable perovskite light-emitting diodes. *Advanced Materials*, 32(25):2000752.
https://doi.org/10.1002/adma.202000752

Zhao XF, Tan ZK, 2020. Large-area near-infrared perovskite light-emitting diodes. *Nature Photonics*, 14(4):215-218.
https://doi.org/10.1038/s41566-019-0559-3

Zheng XP, Yuan S, Liu JK, et al., 2020. Chlorine vacancy passivation in mixed halide perovskite quantum dots by organic pseudohalides enables efficient Rec. 2020 blue light-emitting diodes. *ACS Energy Letters*, 5(3):793-798.
https://doi.org/10.1021/acsenergylett.0c00057

Zhou LF, Yan MX, Luo GJ, et al., 2023. Self-assembled molecule doping enables high-efficiency hole-transport-layer-free perovskite light-emitting diodes. *Advanced Functional Materials*, 33(36):2303370.
https://doi.org/10.1002/adfm.202303370

Zhou YH, Wang CY, Yuan S, et al., 2022. Stabilized low-dimensional species for deep-blue perovskite light-emitting diodes with EQE approaching 3.4%. *Journal of the American Chemical Society*, 144(40):18470-18478.
https://doi.org/10.1021/jacs.2c07172

Zou C, Lin LY, 2020. Effect of emitter orientation on the outcoupling efficiency of perovskite light-emitting diodes. *Optics Letters*, 45(17):4786-4789.
https://doi.org/10.1364/OL.400814

Zou C, Liu Y, Ginger DS, et al., 2020. Suppressing efficiency roll-off at high current densities for ultra-bright green perovskite light-emitting diodes. *ACS Nano*, 14(5):6076-6086.
https://doi.org/10.1021/acsnano.0c01817

Zou Y, Yuan Z, Bai S, et al., 2019. Recent progress toward perovskite light-emitting diodes with enhanced spectral and operational stability. *Materials Today Nano*, 5:100028.
https://doi.org/10.1016/j.mtnano.2019.100028